JOURNAL OF PETROLOGY | VOLUME 38 | NUMBER 7 | PAGES 815–841 | 1997

Igneous and Metamorphic Enclaves in the S-type Deddick Granodiorite, Lachlan Fold Belt, SE Australia: Petrographic, Geochemical and Nd–Sr Isotopic Evidence for Crustal Melting and Magma Mixing

ROLAND MAAS,* IAN A. NICHOLLS AND COLIN LEGG

VIEPS SCHOOL OF EARTH SCIENCES, LA TROBE UNIVERSITY, BUNDOORA, VIC. 3083, AUSTRALIA
VIEPS DEPARTMENT OF EARTH SCIENCES, MONASH UNIVERSITY, CLAYTON, VIC. 3186, AUSTRALIA

RECEIVED APRIL 29, 1996 REVISED TYPESCRIPT ACCEPTED JANUARY 28, 1997

The Deddick Granodiorite, a mafic S-type pluton in the Lachlan Fold Belt, contains abundant enclaves. Most are derived from high-grade metasediments of pelitic–psammitic composition, and migmatites are common. Among these, discrete fragments of melanosomes rich in cordierite and garnet are restites from partial melting. However, compositional and Nd–Sr isotopic data indicate they are not restite in equilibrium with the melt component of the host magma, but may have formed part of a spectrum of diverse magma source lithologies. Alternatively, they may be accidental xenoliths. Regardless of their origin, data for these enclaves suggest their precursors could represent deeply buried age equivalents of the ubiquitous Ordovician turbidites of the Lachlan Fold Belt. Three types of microgranular enclaves with igneous textures are distinguished. The most common type are small and rounded mafic enclaves of tonalitic composition. They carry xenocrysts derived from the host magma, and some contain high-Mg pyroxene derived from a mafic magma. Isotopic data form an array with ε_{Nd} *from –6 to –12, and* $^{87}Sr/^{86}Sr$ *from 0·7130 to 0·7167 (host rock –10 and 0·715, respectively). These enclaves formed as globules of hybrid mafic magma commingled with, and contaminated by, the more felsic host magma. Other enclave types were derived from disrupted syn-plutonic dykes having a distinct isotopic composition, and from a cogenetic marginal facies of the host.*

KEY WORDS: *enclaves; magma mixing; xenocrysts; Nd–Sr isotopes; S-type granites; Lachlan Fold Belt*

INTRODUCTION

Enclaves in granites and volcanic rocks can provide petrogenetic information not readily available from their host rocks (Didier, 1973; Didier & Barbarin, 1991). For example, metasedimentary enclaves can place constraints on the age, composition and deformational history of magma source regions within continental crust (Fleming, 1991; Steele *et al.*, 1991). Enclaves formed by accumulation of early phenocrysts ('autoliths') document the early evolution of the host magma, whereas others may represent commingled magmas and illustrate the possible role of hybridization (Didier, 1987).

Enclave suites in the relatively mafic S-type granitoids of SE Australia are often diverse, including abundant enclaves of metasedimentary origin and microgranular enclaves (Phillips *et al.*, 1981; Price, 1983; Chen *et al.*, 1989; Wyborn *et al.*, 1991). The metasedimentary enclaves are lithologically diverse, including gneissic–migmatitic types and biotite-rich 'surmicaceous' types. Apart from their potential as indicators of crustal structure and composition, they are of interest as possible fragments of source material and/or refractory residue from which peraluminous melts were generated and extracted. By contrast, the microgranular enclaves often have igneous microstructures and generally show strong affinities with their host rocks in terms of mineralogy, mineral composition and bulk chemistry (Didier, 1973; Vernon, 1983).

*Corresponding author. Telephone: 61 (03) 9479 2490. Fax: (03) 9479 1272. e-mail: rmaas@mojave.geol.latrobe.edu.au

Microgranular enclaves in granitoids have been interpreted as (1) 'cognate' fragments of cumulates or wall-rock facies closely related to host magma (e.g. Wall *et al.*, 1987), (2) globules of more mafic, typically hybrid magma commingled with more felsic host magma (Didier, 1973; Vernon, 1984, 1990; Reid & Hamilton, 1987), and (3) fragments of melt residues or of recrystallized, refractory metamorphic rocks from the granite source (Chappell *et al.*, 1987; White *et al.*, 1991). Occasionally, igneous rocks entrained as xenoliths have been reported (see Maury & Didier, 1991). These genetic types may vary between occurrences and conceivably several types could occur in the same pluton, but original distinctions are often destroyed through protracted equilibration of enclaves with felsic host magma (Debon, 1991; Holden *et al.*, 1991). The contrasting interpretations of microgranular enclaves obviously bear on the origin of chemical and isotopic heterogeneities observed within and between many S-type granites and granite suites, as well as in peraluminous volcanics. Such heterogeneities have been attributed to partial melting of mixed sources (McCulloch & Chappell, 1982; Juteau *et al.*, 1986), to magma hybridization (Feldstein *et al.*, 1994; Moreno-Ventas *et al.*, 1995) or to wall-rock assimilation (Lee & Christiansen, 1983).

This study describes a diverse suite of metasedimentary and microgranular enclaves in a particularly enclave-rich S-type granite of the Lachlan Fold Belt, SE Australia, and attempts to identify their origin and their significance in the evolution of the host pluton. In earlier enclave studies in the Lachlan Fold Belt, all enclaves (including microgranular types) present in S-type granitoids have been interpreted as metamorphic rocks derived from the granite source (Chen *et al.*, 1989; White *et al.*, 1991). Other workers, however, have reported evidence for magma mixing in microgranular enclaves in S-type granitoids consistent with an origin as commingled mafic magma globules (Vernon, 1983; Elburg & Nicholls, 1995; Elburg, 1996*a*). The microgranular enclaves described here appear to be only mildly affected by equilibration with the host magma, and preserve compelling mineralogical and isotopic evidence to support the latter studies.

GEOLOGICAL SETTING

The Silurian Deddick Granodiorite (syn. McKillops Bridge Granodiorite, White & Chappell, 1988) is a cordierite-bearing, mafic peraluminous (S-type) pluton in the southern Lachlan Fold Belt, SE Australia. It covers ~100 km^2 in the southermost part of the Kosciusko Batholith in eastern Victoria (Fig. 1) and was emplaced into folded Ordovician to Early Silurian shales and turbidites. The sediments form part of the Yalmy fold and thrust belt in the Canberra–Buchan zone (Glen, 1992). Deformation and metamorphism in the sediments predate the pluton, which is unfoliated [although strongly fractured in places (Ringwood, 1955)] and surrounded by a contact aureole which overprints earlier very low grade greenschist-facies assemblages in the Early Silurian turbidites (Glen & Vandenberg, 1987; Gray, 1988). Several other, similar intrusions occur nearby (e.g. Amboyne, Suggan Buggan, Nunniong Granodiorites) but their occurrence is abruptly terminated to the east at the Yalmy Fault Zone, which in this area is coincident with the I–S line of White & Chappell (1983), thought to mark the eastern termination of thick continental basement. Coeval intrusions of I-type character or more mafic rocks such as gabbros or mafic dykes are not known in the immediate area. The Deddick Granodiorite and its host sediments are unconformably overlain by the Early Devonian andesitic–rhyolitic Snowy River Volcanics which have been gently folded and fractured in the Mid-Devonian (Gray, 1988). Tectonic reconstructions (e.g. Powell, 1984) for the Silurian suggest that the area formed part of a complex back-arc region developed on a fragment of old, rigid continental crust (Chappell *et al.*, 1988; Glen, 1992).

The geochronology of the area is currently being revised, with new SHRIMP U–Pb zircon ages indicating granite ages older than the ~410–415 Ma K–Ar and Rb–Sr mica ages summarized by Richards & Singleton (1981). SHRIMP U–Pb zircon ages around 425–430 Ma have been reported for S-type granitoids in the Kosciusko and Berridale Batholiths (Chappell *et al.*, 1991; Williams, 1992). These ages agree with conventional monazite U–Pb ages reported by Williams *et al.* (1983), who suggested that widespread 410–415 Ma resetting of mica K–Ar and Rb–Sr ages for S-types could be related to I-type magmatism around that time. We have obtained a 425 ± 2 Ma Rb–Sr isochron age from a leaching experiment on biotite from the Deddick Granodiorite (see Table 5, below), consistent with SHRIMP zircon ages for this (new unpublished data) and other S-type granitoids.

The Deddick Granodiorite (see Fig. 1) is representative of numerous strongly peraluminous, cordierite-bearing mafic granitoids of similar age (Chappell & White, 1992) in the Lachlan Fold Belt, e.g. the neighbouring Amboyne and Suggan Buggan Granodiorites (Fig. 1; see also White & Chappell, 1988), the Jillamatong Granodiorite, or the Cowra Granodiorite (Vernon, 1983, 1990; Chen *et al.*, 1989; Wyborn *et al.*, 1991). Like other mafic S-types, the Deddick Granodiorite contains abundant enclaves ranging in size from <2 cm to 1 m. Because of poor outcrop and weathering, detailed observation of enclaves and their distribution is restricted to fresh exposures along the Snowy and Deddick Rivers (Fig. 1). In this area, enclaves make up 4–7 vol. % of the exposure and are more or less uniformly distributed, with the exception

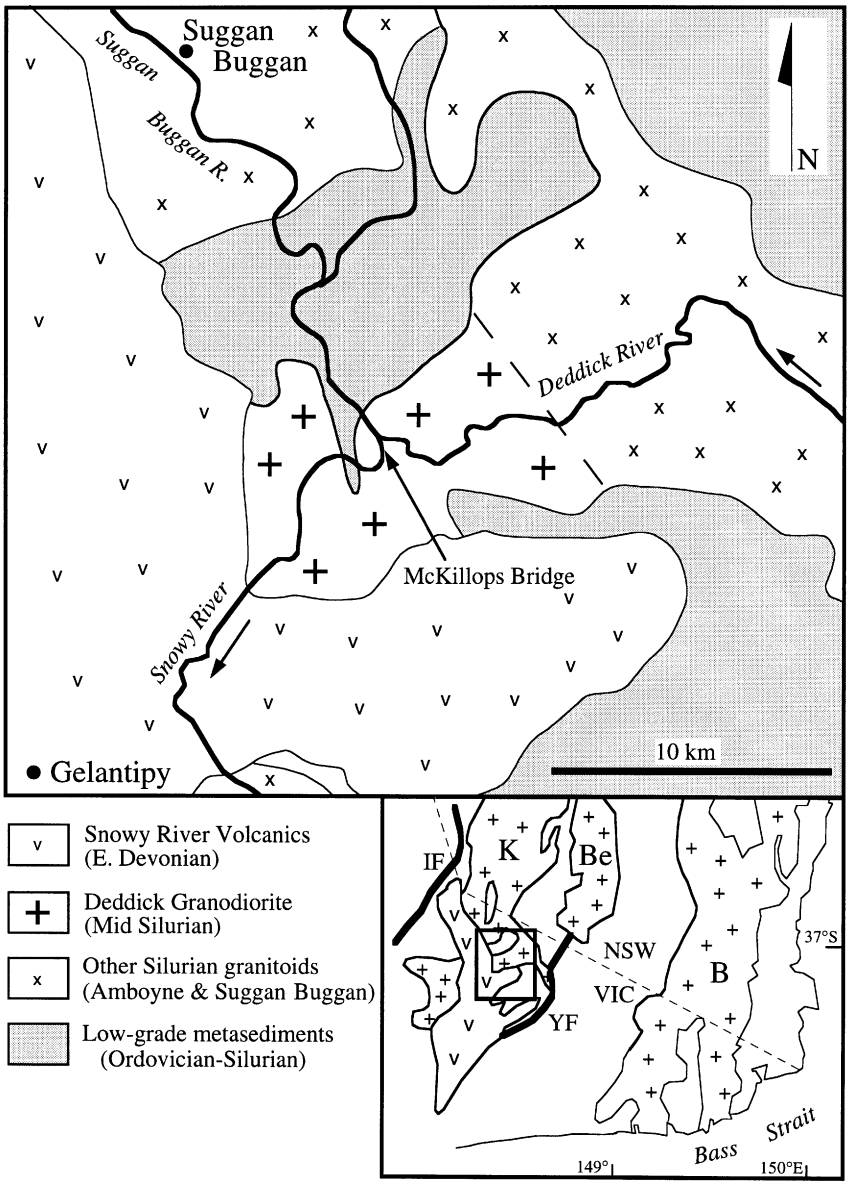

Fig. 1. Simplified geological map of the southern Kosciusko Batholith showing Deddick Granodiorite and sampling area along the Snowy and Deddick Rivers near McKillops Bridge. Geological boundary between the Deddick and Amboyne Granodiorites is poorly known and schematic. Small map shows large-scale geological features of SE Australia, small rectangle is area covered by large map. B, Bega Batholith; Be, Berridale Batholith; IF, Indi Fault; K, Kosciusko Batholith; NSW, New South Wales; VIC, Victoria; YF, Yalmy Fault.

of one of the microgranular types which occurs in rare zones intruded by narrow dykes of granitoid composition (Legg, 1988). The majority of the enclaves have gneissic to migmatitic textures and are rich in biotite and Al-rich minerals, suggestive of a metasedimentary origin. By far the most common type amongst these enclaves are discrete fragments of melanosome material composed of cordierite and garnet, with minor spinel and aluminosilicates. To distinguish them from the gneissic and migmatitic types, they will be referred to as cordierite–garnet enclaves. Other enclave types are subordinate in abundance and include small but ubiquitous quartz–cordierite enclaves, quartz lumps, microgranular enclaves, and hornfelsic xenoliths.

Field relationships and mineralogy

Host granodiorite

The Deddick Granodiorite host phase has a strongly peraluminous mineral assemblage (biotite + cordierite +

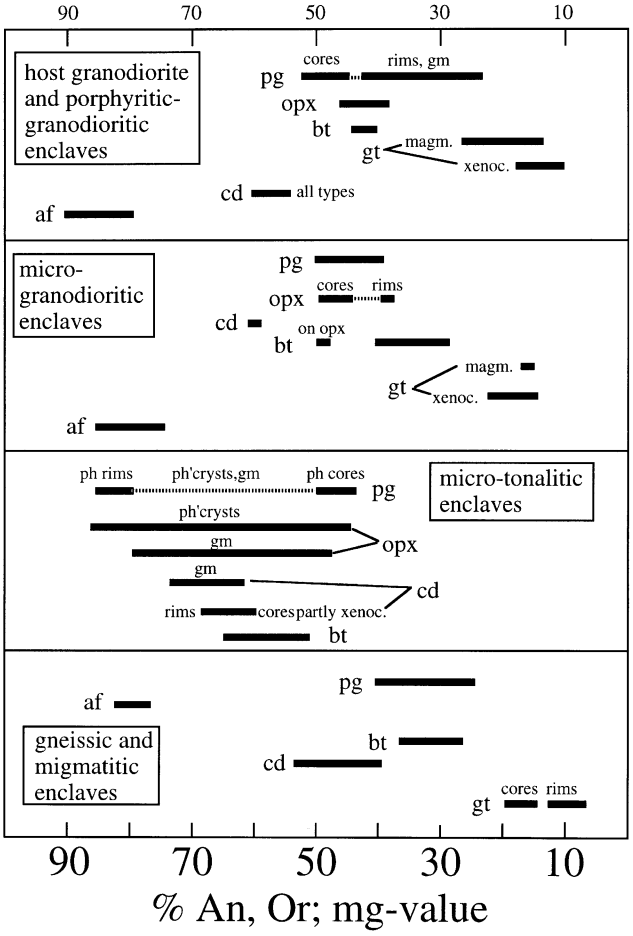

Fig. 2. Compositional ranges in rock-foming minerals in the Deddick granodiorite and its major enclave types. The *x*-axis gives per cent anorthite (pg), per cent orthoclase (af), or $100Mg/Mg+Fe_t$ (opx, bt, gt, cd). (For abbreviations, see Table 1.)

garnet) and high normative corundum (2·4–4·7% C). It is often slightly porphyritic, with rare coarse plagioclase, cordierite and reaction-rimmed garnets (to 20 mm) set in a groundmass of medium (3–5 mm) grainsize. Quartz is the major felsic mineral, followed by plagioclase and subordinate alkali feldspar. Biotite and cordierite typically occur in centimetre-sized clots and are often partially converted to chlorite, muscovite or a mixture of the two ('pinite' after cordierite). Rare orthopyroxene is frequently partially replaced by biotite and quartz.

Gneissic, migmatitic and cordierite–garnet enclaves; quartz–cordierite enclaves

These types make up 80–95% of all observed enclaves and are uniformly distributed over the outcrop area. They vary widely in size (<1 to 50 cm), shape (rounded to angular and irregular), lithology and structure. All have coarse-grained, high-grade metamorphic mineral assemblages, rich in sillimanite, corundum and Zn-rich hercynitic spinel, but lacking orthopyroxene, that distinguish them from superficially similar enclaves with hornfelsic textures (see below).

In the gneissic enclaves, pelitic layers rich in biotite with subordinate cordierite, fibrous sillimanite and rare coarse garnet, alternate with psammitic layers rich in quartz but with lower, highly variable proportions of plagioclase and alkali feldspar. In the migmatitic enclaves, lenticular and patchy leucosomes (≤ 10 mm in width) are developed mainly within biotite-rich layers. Leucosomes may be folded, with axial planes parallel to gneissic layering. Melanosomes are rich in cordierite, garnet and biotite. Discrete cordierite–garnet enclaves are similar to the melanosomes in migmatitic types, typically <10 cm in size and are often found in various stages of disaggregation. Mineral assemblages are dominated by porphyroblastic cordierite (up to 80 vol. %) with abundant inclusions of sillimanite, spinel and corundum, variable proportions of garnet (0–20%), and some examples carry coarse andalusite, in addition to prismatic sillimanite.

Ubiquitous, discrete quartz–cordierite enclaves are small (<10 cm), irregular or rounded, and consist of subequal proportions of quartz and cordierite with minor biotite, sillimanite and zircon. The smallest (<1 cm) may have the external form of single euhedral cordierite crystals. Similar material occurs as rinds on some metasedimentary enclaves, suggesting an origin by reaction between these and the host magma.

Hornfels xenoliths

Irregular blocks of quartzofeldspathic and pelitic material occur near the pluton margins and many are clearly derived from the local wall rocks. Most are undeformed and show characteristic fine equigranular (~0·1 mm) mosaic textures, with quartz, cordierite and biotite dominant in both quartzofeldspathic and pelitic examples. Cordierite is intergrown with variable proportions of alkali feldspar and plagioclase. Orthopyroxene in addition to biotite is present in the margins of some specimens. Others have weak schistosity and appear transitional to the gneissic–migmatitic enclaves, suggesting derivation from metasedimentary precursors over a range of depths.

Microgranular enclaves

Three types of microgranular enclaves could be distinguished. The micro-granodioritic enclaves (~1% of all enclaves) form large blocks from 20 cm to >100 cm in largest dimension, and have angular to slightly rounded outlines. Contacts with the host granodiorite are often slightly crenulated but always sharp. They resemble the host granodiorite mineralogically but have much finer grainsize, slightly more modal plagioclase and biotite but less quartz and alkali feldspar. Rare plagioclase phenocrysts, plagioclase laths, biotite plates, quartz and alkali feldspar occur in weakly poikilitic igneous microstructures. Several examples contain small hypersthene phenocrysts, one has euhedral cordierite and two others have rare coarse garnet, identical to that in the host granodiorite. Occasionally, as near the junction of the Deddick and Snowy Rivers, enclaves of this type can be traced to dismembered, >1 m wide synplutonic dykes.

The micro-tonalitic enclaves are mostly small (<10 cm) and have ovoid to sub-spherical shapes. They make up 1–3% of all enclaves but occasionally occur in greater abundance within polygenetic swarms surrounded by unusually leucocratic host granite. The enclaves are typically homogeneous, fine grained and have equigranular, weakly poikilitic igneous microstructures. One important example carries phenocrysts of plagioclase and hypersthene. Most are dominated by the assemblage plagioclase + biotite + hypersthene + quartz, with two examples containing relatively abundant cordierite and one containing salitic clinopyroxene and garnet. Two examples are zoned, with cores that contain hypersthene and actinolite (presumably after Ca-clinopyroxene), but no biotite. The rims resemble other, unzoned enclaves, containing hypersthene, biotite, plagioclase and quartz in roughly equal proportions.

The rare porphyritic granodiorite enclaves consist of phenocrysts of plagioclase, cordierite, quartz and biotite, almost identical in size, habit and composition to the same minerals in the host, set in a fine-grained (<0·5 mm) groundmass. Apatites occurring in the groundmass have an acicular habit. The enclaves strongly resemble thick (10 cm) rinds of weakly porphyritic granodiorite developed on some hornfelsic xenoliths.

Petrography and mineral chemistry

Petrographic and mineral chemical data for the Deddick Granodiorite and its enclaves are compiled in Table 1, and representative mineral compositions are listed in Tables 2 and 3. The following sections describe some of the key features of these rocks.

Deddick Granodiorite

Plagioclase typically consists of broad, often altered cores showing oscillatory and patchy zoning over a small range of compositions ($An_{52–45}$), surrounded by narrow rims, strongly zoned to An_{24} (for abbreviations refer to Table 1). Biotite occurs as red–brown, euhedral–subhedral plates up to 3 mm or, more commonly, in clots up to 15 mm in size, and typically has high TiO_2 contents. Plagioclase and biotite crystals similar to those described here are common in S-type granitoids (e.g. Hine *et al.*, 1978). Cordierite forms coarse euhedral crystals with few inclusions and resembles the magmatic cordierite found in other S-type granitoids (Chappell & White, 1992). A second distinct type of cordierite of similar composition forms anhedral grains rich in inclusions of hercynite and fibrous sillimanite. Inclusion-rich cordierite of this type is commonly overgrown by euhedral, clear, magmatic cordierite. The inclusion-rich cordierite strongly resembles the less magnesian cordierite typical of the metasedimentary enclaves (see below) and may be xenocrystic. Garnet also occurs in two distinct types. The more common garnet type forms coarse (1–20 mm) euhedral, almandine-rich grains with relatively few inclusions, uniform in composition apart from narrow peripheral zones of high spessartine–almandine and lower pyrope component. A second type of almandine-rich garnet occurs as coarse, anhedral grains often containing a core crowded with tiny mineral and fluid inclusions, and showing complex zoning. Inclusion-rich garnet of this type is sometimes rimmed by clear, euhedral (magmatic) garnet of the first type. Very similar inclusion-rich garnets occur in the high-grade metasedimentary enclaves and their counterparts in the host granodiorite may therefore

Table 1: Summary of petrographic observations and mineral chemical data for the Deddick Granodiorite and its enclaves

Rock type:	Host granodiorite & porphyr. grd. enclaves	Metasedimentary enclaves			Microtonalitic enclaves	Microgranodior. enclaves
		gneissic–migmatitic	cordierite–garnet	quartz–cordierite		
Assemblage:	qz pg af bt cd gt ± opx cd gt sill hc	qz af pg bt and cor hc	cd gt bt sill	qz cd bt sill zr	pg bt opx qz ± cd–cpx–gt	pg bt qz af ± cd ± opx ± gt
quartz	35–40% subhedral–ovoid rare incl. of bt pg ap zr common fluid incl.	up to 80% in felsic, 10–30% in bt-rich layers 0·1–5 mm granoblastic–xenoblastic	rare	47–55%, 1–5 mm poikilitically enclosed in cd megacryst	interstitial, ocelli to 5 mm rimmed with opx + pg	poikilitic–interstitial
plagioclase	25–30% phenocrysts subhedral tabular, altered cores $An_{52–45}$, thin rims An_{24}, matrix low-An to An_{42}	1 mm, common w. qz + af in gneisses but rare in leucosomes, $An_{40–25}$ locally incl. of sill	minor, $An_{40–25}$	absent	phenocrysts to 5 mm cores An_{50}, intermed. zones with melt incl., rims to An_{85} g'mass pg $An_{80–50}$	phenocrysts to 3 mm An_{50} g'mass <1 mm laths $An_{50–40}$
alkali feldspar	9–14% interstitial	1 mm, with qz + pg in felsic layers, with qz in leucosomes	v. rare	absent	absent	interstitial
biotite	11–17% clots to 15 mm red–brown to yellow pleochroism, 4·5–6% TiO_2, $Mg_{44–41}$	70–80% in bt-rich layers decreasing in melanos. $Mg_{36–27}$, 4–7% TiO_2	minor	<10%, platy crystals	<0·5 mm euhedral plates in g'mass, 3·5–5·5% TiO_2 $Mg_{65–51}$	<0·5 mm sub-hexagonal plates red–brown pleochroism as in host, $Mg_{40–29}$

cordierite	5–10%, to 10 mm magmatic: coarse, euhedral, few incl.(pg) xenocrystic: coarse, anhedral, incl. of fibrous sill, hc, bt, ap, zr; all types $Mg_{60–50}$	coarse, anhedral, many incl. of sill, hc, bt $Mg_{52–40}$, mostly $Mg_{48–44}$	up to 80%, euhedral, many incl. of sill, hc, cor	46–38%, often megacrysts sieved with qz, bt, sill, zr	rare xenocrysts to 5 mm (60540A, D1, 8499B), reaction rims (pg–bt), incl. of sill needles reverse zoning $Mg_{62–67}$; magmatic g'mass 0·1–0·5 mm, $Mg_{74–66}$	v. rare (B15), magmatic similar to cd in host gd.
garnet	<0·1%, round-subhed., magmatic: 1–15 mm, subhedral, clear, $Mg_{25–15}$ xenocrystic: anhedral, rare incl., $Mg_{17–11}$; often core with many incl. (qz, il, fluid) $Mg_{19–15}$ all types alm-rich	rare in gneisses, more common in melanos. (see residual encl.)	0–20% alm-rich incl. free $Mg_{17–7}$ often w. core rich in incl. (qz il fluid) $Mg_{19–15}$	absent	v. rare (only in J2) xenocrystic magmatic gt from host gd., reaction rim (pg–opx)	rare xenocrysts; w. sill incl. in B15; w. core full of incl. in K2
orthopyroxene	<0·5%, magmatic: euhedral–subhedral, $Mg_{46–39}$; also secondary in opx+bt+cd after gt	absent	absent	absent	phenocrysts 1–3 mm euhedral prisms, normal zoning, cores to Mg_{85}, rims to Mg_{46}; g'mass <0·1 to 0·5 mm, euhedral $Mg_{60–50}$	rare euhedral phenocrysts >1 mm in F12, K2, B22 zoned $Mg_{49–37}$
other	trace il, ap, zr, ru, po; sill, hc incl. in cd	fibrous sill in cd, pg	fibrous sill in cd, coarse idioblastic sil+and	coarse sill prisms	rare Ca-cpx (J2); act in bt-free cores of zoned encl. (Z4, 8318) g'mass has acicular ap, il, zr	acicular ap in qz pools

incl., mineral or fluid inclusions in other mineral; g'mass, groundmass; subhed., subhedral; pg, plagioclase; qz, quartz; af, alkali feldspar; bt, biotite; cd, cordierite; gt, garnet; opx, orthopyroxene; sill, sillimanite; act, actinolite; and, andalusite; hc, hercynite spinel; cor, corundum; alm, almandine; ap, apatite; il, ilmenite; zr, zircon; cpx, clinopyroxene; po, pyrrhotite; ru, rutile; Mg_{85}, cation ratio $100Mg/(Mg+Fe_t)$; An_{50}, per cent anorthite in plagioclase.

Table 2: Selected pyroxene analyses: Deddick Granodiorite and its enclaves

	opx	opx	opx	opx	opx	opx	opx	opx	opx	opx	cpx
Sample:	B21	B21	F7	F12	F12	60540a	60540a	60540a	D1	J2	J2
Type:	pc core	pc-rim	pc-core	pc-core	pc-rim	pc	gm	gm	pc	pc	cpx-core
Rock:	host	host	host	microgranular enclaves							
SiO_2	48·13	47·59	48·55	49·45	48·39	55·81	54·62	51·21	51·04	53·01	52·49
TiO_2	0·12	0·00	0·22	0·00	0·24	0·00	0·08	0·17	0·07	0·23	0·00
Al_2O_3	1·24	3·04	2·63	2·00	1·12	1·09	2·04	0·76	1·65	1·25	0·25
Cr_2O_3	0·00	0·00	0·00	0·00	0·00	0·43	0·09	0·00	0·27	0·18	0·11
FeO_t	36·09	34·71	1·68	31·64	36·38	10·09	12·85	29·66	26·88	19·91	10·66
MnO	1·30	1·03	0·74	1·09	1·59	0·13	0·23	0·66	0·69	0·45	0·00
MgO	12·95	12·56	31·74	15·55	11·93	31·20	27·87	17·04	19·02	22·81	13·25
CaO	0·18	0·16	0·22	0·21	0·36	1·26	2·22	0·33	0·38	2·16	23·25
Cations											
no. O	6	6	6	6	6	6	6	6	6	6	6
Si	1·941	1·912	1·908	1·936	1·949	1·964	1·951	1·979	1·948	1·962	1·979
Al	0·080	0·144	0·122	0·092	0·053	0·045	0·086	0·035	0·074	0·055	0·011
Cr	0·000	0·000	0·000	0·000	0·000	0·012	0·002	0·000	0·008	0·005	0·003
Ti	0·002	0·000	0·007	0·000	0·007	0·000	0·002	0·006	0·002	0·006	0·000
Fe	1·186	1·166	1·093	1·036	1·224	0·297	0·384	0·959	0·858	0·616	0·336
Mn	0·047	0·035	0·025	0·036	0·054	0·004	0·007	0·022	0·022	0·014	0·000
Mg	0·757	0·752	0·837	0·908	0·716	1·637	1·484	0·982	1·082	1·258	0·754
Ca	0·006	0·007	0·009	0·009	0·016	0·048	0·085	0·014	0·016	0·086	0·939
mg-no.	39	39	43	47	37	85	79	51	56	67	69

F12 is from a granodioritic dyke related to the micro-granodioritic enclaves; 60540a, D1 and J2 are micro-tonalitic enclaves. pc, phenocryst; gm, groundmass; cpx, clinopyroxene in sample J2, other analyses are orthopyroxene.

Table 3: Selected mineral analyses: Deddick Granodiorite and its enclaves

	biotite	biotite	biotite	biotite	biotite	biotite	biotite	biotite	biotite	biotite	garnet	garnet
Sample:	B21	F7	F12	B15	B22	D1	60540a	I2R	8509	C1C1	C1C1	F7
Type:	pc	pc			gm	pc					rim	core
Rock:	host	host	micro-granitoid enclaves					metasedimentary enclaves			host	
SiO_2	34·93	35·21	34·34	34·59	35·40	37·39	36·11	34·68	34·22	34·47	36·93	37·41
TiO_2	4·95	5·98	3·91	4·80	4·33	3·59	5·54	3·96	4·83	4·89	0·00	0·00
Al_2O_3	15·21	15·63	15·00	15·59	16·01	15·57	15·17	16·96	17·11	17·55	21·23	21·83
FeO_t	21·23	22·09	27·55	24·00	22·02	14·52	19·16	24·02	25·61	22·45	31·77	30·01
MnO	0·00	0·10	0·23	0·22	0·03	0·08	0·00	0·00	0·00	0·11	5·31	3·07
MgO	8·94	8·71	6·26	7·37	8·27	14·76	11·21	6·48	5·43	7·19	3·50	5·36
CaO	0·00	0·00	0·00	0·00	0·00	0·00	0·00	0·00	0·00	0·00	1·25	1·99
Na_2O	0·30	0·32	0·08	0·16	0·19	0·19	0·21	0·00	0·29	0·41	0·00	0·00
K_2O	8·93	9·36	9·08	8·81	9·22	9·35	9·29	9·32	9·29	9·34	0·00	0·00
Total	94·49	97·41	96·45	95·54	95·47	95·45	96·69	95·42	96·78	96·41	100·08	99·73
Cations												
no. O	22	22	22	22	22	22	22	22	22	22	24	24
Si	5·440	5·346	5·415	5·398	5·467	5·556	5·433	5·412	5·314	5·293	5·934	5·928
Al IV	2·560	2·654	2·585	2·602	2·533	2·444	2·567	2·588	2·686	2·707	0·066	0·072
Al VI	0·232	0·144	0·203	0·265	0·381	0·282	0·122	0·530	0·445	0·470	3·956	4·006
Ti	0·580	0·682	0·464	0·563	0·503	0·401	0·627	0·465	0·564	0·565	0·000	0·000
Fe	2·765	2·804	3·633	3·132	2·844	1·804	2·410	3·134	3·326	2·883	4·270	1·988
Mn	0·000	0·013	0·031	0·029	0·004	0·010	0·000	0·000	0·000	0·014	0·722	0·412
Mg	2·076	1·972	1·472	1·715	1·904	3·269	2·514	1·507	1·257	1·646	0·838	1·266
Ca	0·000	0·000	0·000	0·000	0·000	0·000	0·000	0·000	0·000	0·000	0·216	0·338
Na	0·091	0·094	0·024	0·048	0·057	0·055	0·061	0·000	0·087	0·122	0·000	0·000
K	1·774	1·816	1·827	1·754	1·816	1·772	1·783	1·855	1·840	1·830	0·000	0·000
mg-no.	43	41	29	35	40	64	51	32	27	36	16	39

B15 and B22 are micro-granodioritic enclaves, and F12 is a dyke related to the former; 60540a and D1 are micro-tonalitic enclaves; I2R and 8509 are cordierite–garnet enclaves; C1C1 is a gneissic enclave. pc, phenocryst; gm, groundmass. F7 garnet (plus F7 orthopyroxene, see Table 2, and plagioclase, An_{25}) used for *P–T* estimate for host granodiorite. C1C1 garnet (rim inwards of zone of retrograde Mn diffusion) and plagioclase (An_{40}) used for *P* estimate for gneissic enclaves.

be xenocrystic. Both magmatic and xenocrystic garnet were unstable under the conditions of final emplacement and cooling and have developed reaction coronas (cd–bt–opx). The compositions of the four coexisting ferromagnesian phases (Table 1) form a trend ($Mg_{cordierite}>Mg_{biotite}>Mg_{orthopyroxene}>Mg_{garnet}$) also noted in S-type volcanics of the Lachlan Fold Belt (Wyborn *et al.*, 1981; Clemens & Wall, 1984); this trend is considered to be typical of metamorphic equilibrium assemblages (e.g. Hoffer & Grant, 1980).

High-grade metasedimentary enclaves

Plagioclase is common only in the gneissic enclaves, where it forms unzoned to weakly zoned xenomorphic crystals with occasional inclusions of fibrous sillimanite. Xenomorphic cordierite is abundant in pelitic portions of the gneissic enclaves and may form 80% of the mode in migmatite melanosomes and cordierite–garnet enclaves. Common inclusions in cordierite are green hercynitic spinel, folded bundles of fibrous sillimanite, occasional biotite, and—in the cordierite–garnet inclusions and in migmatite melanosomes—corundum. Relict biotite and sillimanite may derive from the cordierite-forming reaction $bt + sill + qz = cord + kf + H_2O$. Garnet forms idiomorphic to xenomorphic grains of 1–10 mm, often comprising a large core riddled with mineral (ilmenite, quartz) and fluid inclusions, and rims without fluid inclusions but containing biotite and sillimanite. The garnets are almandine rich and exhibit complex bell-shaped Mg–Fe–Mn–Ca zoning patterns related to their metamorphic growth history (Legg, 1988). Garnets in the gneissic enclaves are usually unreacted whereas similar garnets in migmatitic melanosomes and in cordierite–garnet enclaves have symplectitic reaction coronas (bt–cd–hc–cor). Other minerals in the cordierite–garnet enclaves include rare quartz, K-feldspar and plagioclase; the last of these is never in contact with other felsic minerals. Sillimanite occurs chiefly as inclusions in cordierite but is coarse grained and prismatic in those cordierite–garnet enclaves that carry andalusite. The latter is restricted to the most aluminous enclaves, is coarse grained, idioblastic and inclusion free, but often reacted to cordierite + spinel + corundum. Biotite is far less abundant in the cordierite–garnet enclaves than in the gneissic enclaves, reflecting breakdown of biotite to yield felsic leucosome melt.

Mineral compositions are similar throughout the range of enclave types described above. Relative to their counterparts in the host granodiorite, plagioclase in the enclaves is less calcic ($An_{25–40}$) and mafic minerals are commonly more Fe rich (primary biotite $Mg_{36–27}$; cordierite $Mg_{53–40}$). A similar relationship was noted for metasedimentary enclaves in other peraluminous granitoids in SE Australia and in the Massif Central (Chen *et al.*, 1989; Montel *et al.*, 1991).

Microgranular enclaves

The micro-granodioritic enclaves contain the same type of TiO_2-rich biotite as the host granodiorite but compositions vary more widely, from Mg_{40} in the most mafic sample (B22) to $Mg_{28–30}$ in the least mafic sample (F12). Rare euhedral orthopyroxene is partially replaced by chlorite or fine clays, shows normal zonation and has higher *mg*-number ($Mg_{49–37}$) than coexisting biotite. This differs from the equilibrium situation ($Mg_{bt} \geq Mg_{opx}$) observed in the host granodiorite and in the porphyritic granodiorite enclaves (Table 1). Cordierite has only been observed in enclave B15, where it forms euhedral, unreacted magmatic crystals. Garnet is absent except for single garnet crystals rich in mineral inclusions found in enclaves B15 and K2. They carry reaction coronas of (pg–opx) or (pg–bt), respectively, but otherwise resemble garnets in the host rock and in the metasedimentary enclaves and are probably xenocrysts.

The micro-tonalitic enclaves show considerable mineralogical variability and evidence of disequilibrium. Plagioclase phenocrysts have cores similar in size and composition ($\sim An_{50}$) to plagioclase in the host granodiorite, rimmed by more calcic plagioclase ($An_{80–85}$). Some grains have core–rim transition zones zones riddled with melt inclusions, of the type produced by Tsuchiyama (1985) by reacting sodic plagioclase with calcic melt. Fine-grained plagioclase in the groundmass is also anorthite rich ($An_{80–50}$). Quartz occurs largely in the groundmass, where it poikilitically encloses all other minerals. However, corroded quartz grains up to 5 mm in diameter, with prominent (pg–opx) reaction rims, occur in most samples. They resemble the quartz 'ocelli' described from many mafic micro-granular enclave suites (e.g. Vernon, 1990). Biotite shows broad ranges in *mg*-number ($Mg_{65–51}$) and TiO_2 content (3·6–5·6%), even within a single enclave, and is considerably more magnesian than biotite in the host rock or in other enclave types. Orthopyroxene forms euhedral phenocrysts which may occur in glomeroporphyritic clots, and as tiny ($\leq 0·5$ mm) perfect prisms in the groundmass. Phenocrysts may be strongly optically zoned with very magnesian cores. For example, enclave 60540A has bronzite ($Mg_{85–82}$) cores surrounded by narrow rims of hypersthene ($Mg_{60–55}$). Groundmass hypersthene prisms in 60540A are highly variable in composition ($Mg_{79–51}$). In enclave J2, orthopyroxene compositions show a smaller range ($Mg_{67–49}$). In this sample, a small crystal clot (<1 mm) has been found, consisting of hypersthene, normally zoned Ca-clinopyroxene ($Mg_{69–59}$), plagioclase and quartz, with clinopyroxene forming thin mantles on hypersthene prism faces. Similar features are common in natural and experimental andesitic assemblages; however, only one example has been found in this study. Relatively coarse-grained (to 5 mm) cordierite occurs in several samples. Enclave 60540A carries rare

inclusion-free cordierite showing reverse zoning, from Mg_{61} cores to Mg_{67} rims. The cores of these grains are compositionally similar to the magmatic cordierite from the host granodiorite ($Mg_{60–55}$), whereas the rim compositions match those of fine-grained cordierite (Mg_{66}) elsewhere in the enclave. Coarse cordierites in enclaves 8499B and D1 are relatively magnesian (Mg_{66}), and often carry sillimanite needles. They may represent adjusted xenocrystic cordierite ultimately derived from the metasedimentary enclaves. Rim and groundmass cordierites in these two enclaves are again more magnesian ($Mg_{74–69}$) and in textural equilibrium with quartz, suggestive of a magmatic origin. Almost all cordierites are strongly corroded and variably replaced by plagioclase + green biotite; clots of plagioclase + green biotite in apparently cordierite-free micro-tonalite enclaves may represent cordierite pseudomorphs. A single garnet with a (pg–opx) reaction rim occurs in enclave J2; the grain strongly resembles the magmatic almandine in the host. Acicular apatites are common in the groundmass.

CONDITIONS OF CRYSTALLIZATION AND EMPLACEMENT

Pressure–temperature estimates for the early stages of crystallization of the host magma were derived from Fe–Mg exchange equilibria in coexisting orthopyroxene and garnet, using the calibrations of (for temperature) Harley (1984), Sen & Bhattacharya (1984) and Lee & Ganguly (1988), and (for pressure) Bohlen *et al.* (1983), Perkins & Chipera (1985), Powell & Holland (1987) and Moecher *et al.* (1988). A rare magmatic intergrowth of orthopyroxene and garnet in sample F7 (mineral data Tables 2 and 3) yields 840 ± 60°C and $0{\cdot}55 \pm 0{\cdot}1$ GPa. Uncertainties reflect the dispersion between different calibrations but do not reflect the much greater uncertainties from other sources (Spear, 1993). However, the results are consistent with P–T estimates for other Lachlan Fold Belt peraluminous felsic complexes (Wyborn *et al.*, 1981; Clemens, 1988) and suggest depths of source melting and early magmatic crystallization of ~20 km. Final emplacement of the host granodiorite probably occurred at depths of <10 km (<0·25 GPa), based on coexisting cordierite + orthopyroxene in hornfels xenoliths.

Inclusion relationships for major minerals of the host granodiorite suggest the crystallization sequence quartz~orthopyroxene–biotite~plagioclase~cordierite–alkali feldspar. If the magma carried minimal restite or xenocrysts, this sequence may be compared with experimental sequences for the compositionally similar Lake Mountain Rhyodacite (Clemens, 1981). In the latter, quartz begins to crystallize at about the same time as orthopyroxene and before plagioclase at 0·5 GPa, but not at 0·2 GPa, and then only at low water activities ($a_{H_2O} \leq 0{\cdot}2$). The experimental sequence at 0·5 GPa, at $a_{H_2O} \sim 0{\cdot}2$, is quartz~orthopyroxene (960°C)–garnet (920°C)–plagioclase (910°C)–biotite (880°C), with orthopyroxene stable to near-solidus temperatures (830°C). These experimental data support the pressure estimate of 0·55 GPa for early crystallization in the granodiorite magma, but suggest temperatures 50–100°C higher than those indicated by mineral geothermometry, presumably because of near-solidus re-equilibration of early-formed minerals.

If the Deddick Granodiorite magma carried significant restite or xenocrysts, a suitable model for crystallization of the liquid component should be provided by the peraluminous Strathbogie Granite composition also studied experimentally by Clemens (1981). In this composition, quartz and orthopyroxene again start to crystallize before plagioclase at 0·5 GPa but not at 0·2 GPa, but to slightly higher a_{H_2O} (0·3) than in the case of the Lake Mountain Rhyodacite. The relevant experimental crystallization sequence for Strathbogie is garnet (940°C)–quartz~orthopyroxene (930°C)–biotite~plagioclase (870°C), with orthopyroxene again stable down to 830°C.

The inferred crystallization sequence for major minerals of the micro-granodioritic enclaves is plagioclase–orthopyroxene–biotite~quartz–alkali feldspar. In enclave B15, large subhedral cordierites apparently began to form before biotite and remained stable, but no magmatic garnet formed. Fe-rich biotite in these enclaves formed late relative to the more Mg-rich biotite in the Deddick Granodiorite host. This sequence is comparable with that determined experimentally for the Lake Mountain Rhyodacite at 0·1 GPa and $a_{H_2O} \sim 0{\cdot}5$ (magma water content 2–3 wt %). Such a low pressure is consistent with the field evidence, such as the partial preservation of original intrusive relationships and the extremely limited mechanical interaction between either enclaves or dykes with the host granodiorite. It also indicates that the levels of the pluton exposed at present may have been as shallow as 4–5 km at the time of emplacement.

The occurrence of partial melting in the high-grade metapelitic enclaves suggests a minimum temperature of 750°C (Clemens & Vielzeuf, 1987), or higher where extensive biotite breakdown to form melt is observed. Garnet–biotite thermometry for a gneissic enclave (sample C1C1, mineral data Tables 2 and 3) yields 820 ± 100°C [(calibrations of Ferry & Spear (1978) with or without garnet solution model of Berman (1990); Hodges & Spear (1982); Ganguly & Saxena (1984); Indares & Martignole (1985)]. This estimate may be biased to some extent by retrograde diffusion rims in garnet which prevent determination of true garnet rim compositions. A pressure of $0{\cdot}55 \pm 1{\cdot}5$ GPa was derived

Table 4: Major and trace element data: Deddick Granodiorite and its enclaves

	Host granodiorite					Metasedimentary enclaves											
						cordierite–quartz				migmatitic			gneissic			qz–cd	hornfels	
Sample:	B21	F7	L1	K3	M13	B25	C29B	C6	8509	I1R	I2leu	I2mel	G2	D6A	C1	C27B	B4	B29
SiO_2	69·27	68·78	69·74	67·59	68·62	50·25	45·33	50·79	46·70	44·92	72·96	44·00	54·82	52·01	53·67	68·74	53·09	52·65
TiO_2	0·62	0·68	0·60	0·70	0·61	1·18	1·29	1·07	1·47	1·40	0·16	1·62	1·28	0·88	1·27	0·65	0·92	0·99
Al_2O_3	14·87	14·92	15·22	15·68	15·41	30·35	31·06	30·14	30·09	31·40	14·75	32·35	23·28	28·51	23·27	16·71	25·09	25·48
FeO_t	4·64	5·03	4·37	5·11	4·90	8·03	12·15	6·14	11·25	12·40	1·12	13·37	8·17	8·08	9·72	6·94	6·51	6·59
MnO	0·11	0·09	0·05	0·08	0·04	0·11	0·31	0·12	0·48	0·42	0·01	0·41	0·09	0·09	0·12	0·12	0·01	0·10
MgO	2·05	2·25	1·99	2·29	2·07	3·44	4·84	1·67	2·49	4·46	0·58	4·05	3·23	3·09	4·00	3·65	3·35	3·26
CaO	2·20	2·41	2·13	2·94	2·02	0·74	1·04	3·11	2·14	1·13	0·59	0·84	0·47	0·67	0·72	0·20	3·16	4·06
Na_2O	2·12	2·04	1·93	2·09	1·79	1·23	1·16	3·12	1·51	1·34	1·97	1·12	1·42	1·24	1·13	0·48	2·91	3·29
K_2O	4·11	3·79	3·95	3·52	4·54	4·67	2·63	3·69	3·69	2·36	7·86	2·23	7·22	5·26	5·98	2·52	4·82	3·59
A/CNK	1·25	1·26	1·35	1·25	1·34	3·60	4·67	2·04	2·90	4·61	1·16	5·59	2·11	3·18	2·41	4·30	1·59	1·53
Na_2O/K_2O	78	0·82	0·74	0·90	0·60	0·40	0·48	1·29	0·62	0·86	0·38	0·76	0·30	0·36	0·29	0·29	0·92	1·39
mg-no.	44	44	45	44	43												46	47
Ba	528	553				1177	661	537	1530	478	1983	504	1408	1308		379	598	416
Rb	183	172	186	163	165	234	217	204	199	161	232	142	319	220	380	205	286	217
Sr	151	150	142	143	126	105	101	263	301	95	231	65	142	156	109	14	237	280
Pb	27	32	33	32	38	30	12	31	29	25	94	14	30	45		3	33	36
Th	15	17	13	21	21	27	30	24	33	33	9	36	25	26	23	21	25	25
Zr	173	168	180	184	178	181	178	134	214	204	22	197	220	137	200	249	111	125
Y	27	30	30	27	35	51	53	31	110	70	13	98	27	39	39	14	36	38
Nb	13	18				19	32	25	31	33	5	40	28	20		12	23	20
La	31	37				72	62	47	70	73	10	95	30	57		38	50	67
Ce	66	62				172	129	92	151	152	18	189	66	117		87	117	140
Sc	13	11				21	22	17	28	26	0	32	17	18		5	14	15
V	96	102				174	172	168	181	205	15	251	160	153		72	143	147
Cr	58	56				150	157	125	141	179	5	223	125	111		58	128	134
Ni	18	22	17	23	20	52	68	39	47	53	10	62	50	49	54	21	38	30

			Microgranular enclaves															
	hornfels		porph.m'grd		micro-granodioritic						micro-tonalitic							
Sample:	B29	8503C	B11	B21B	B22	M1	K2	F12*	M8	B15	8499B	D1	60450a	60540c	A6	A4A	Z4B	J2
SiO_2	55·23	50·97	67·93	67·29	66·94	69·10	67·75	70·15	67·36	67·84	64·97	64·59	62·22	61·83	61·81	56·40	62·49	58·23
TiO_2	0·96	1·55	0·73	0·72	0·94	0·98	1·04	0·98	1·16	0·98	0·49	0·63	0·55	0·50	0·64	1·19	0·94	1·76
Al_2O_3	23·02	22·59	16·65	15·97	16·05	15·14	15·21	14·41	15·25	15·41	14·35	14·61	15·69	15·84	16·66	17·49	16·42	18·06
FeO_t	6·88	13·19	5·27	5·52	4·88	4·59	5·73	4·58	5·40	5·04	7·22	6·99	7·27	8·92	7·02	8·74	7·21	9·07
MnO	0·11	0·18	0·06	0·04	0·09	0·08	0·03	0·06	0·06	0·08	0·15	0·13	0·12	0·17	0·18	0·19	0·10	0·14
MgO	3·25	6·03	2·20	2·57	1·78	1·47	1·55	1·00	1·53	1·49	4·87	5·60	4·97	4·02	4·35	5·97	3·65	2·94
CaO	1·17	0·11	1·77	2·90	3·61	3·23	3·21	3·41	2·46	2·71	4·14	3·85	6·30	5·68	5·40	7·95	5·53	5·56
Na_2O	1·88	0·83	1·92	2·18	2·72	2·42	2·15	2·12	2·34	2·04	2·12	1·90	1·71	1·74	1·21	0·53	1·95	2·04
K_2O	7·35	4·54	4·42	2·72	2·81	2·69	3·29	3·21	4·29	4·32	1·68	1·70	1·16	1·29	2·74	1·49	1·64	2·04
A/CNK	1·75	3·48	1·31	1·35	1·14	1·19	1·18	1·09	1·18	1·19	1·12	1·22	1·01	1·09	1·13	1·03	1·09	1·15
Na_2O/K_2O	0·39	0·28	0·66	1·22	1·47	1·37	0·99	1·00	0·83	0·72	1·92	1·70	2·24	2·05	0·67	0·54	1·81	1·52
mg-no.	46	44	43	45	39	38	33	28	34	35	54	59	55	45	53	55	47	37
Ba	1393	476			504						226	344	312	267				
Rb	365	431	188	178	160	146	171	140	185	163	115	97	73	80	162	119	100	108
Sr	153	27	152	159	196	198	195	120	150	127	184	163	226	239	174	115	286	171
Pb	36	16	35	24	25	28	30	33	33	35	18	14	16	24	15	10	17	21
Th	18	31	24	23	19	22	21	27	20	25	13	15	14	9	10	8	14	17
Zr	156	260	270	176	196	246	212	246	267	243	126	137	124	91	137	148	181	229
Y	35	16	46	31	40	45	44	50	50	40	24	23	23	21	39	37	29	47
Nb	21	30			14						12	14	10	13				
La	39	55			40						24	23	22	27				
Ce	78	121			78						61	60	62	49				
Sc	14	22			11						21	16	25	25				
Cr	109	184			6						283	341	146	130				
Ni	42	69	11	26	8	1	6	7	5	5	62	77	27	32				

Major elements determined by electron microprobe on fused rock powders (Nicholls, 1974). Trace elements (in p.p.m.) by X-ray fluorescence of pressed pellets. A/CNK = molar Al/(Ca + Na + K), calculated for total Ca; *mg*-number = molar Mg/(Mg + Fe_t) × 100. I2leu and I2mel refer to leucosome and melanosome of sample I2, respectively.
*Sample F12 is from a granodioritic dyke related to the micro-granodioritic enclaves.

from the garnet–plagioclase–Al_2SiO_5–quartz geobarometer, using the same garnet analysis and a plagioclase with An_{40} (Newton & Haselton, 1981; Hodges & Spear, 1982; Ganguly & Saxena, 1984; Hodges & Crowley, 1985; Kozial, 1989). Garnet, biotite and plagioclase compositions in the other metasedimentary enclave types do not vary greatly from those in C1C1, suggesting that they record similar P–T conditions. These indicate equilibration depths close to those suggested for early crystallization of the host magma. However, the presence of primary andalusite in some cordierite–garnet enclaves suggests their derivation from slightly shallower depths (~15 km), with a loose upper limit provided by the varied estimates of the Al_2SiO_5 triple point pressure, taken here as ~0·4 GPa (Holdaway, 1971; Salje & Wernecke, 1982).

WHOLE-ROCK GEOCHEMISTRY AND Nd–Sr ISOTOPES

The Deddick Granodiorite shows the high SiO_2, total FeO (FeO_t) and MgO, and low Na_2O/K_2O ratios (Table 4) that are typical of mafic peraluminous granitoids of the Lachlan Fold Belt (Chappell & White, 1992). Its enclaves are all peraluminous, have FeO_t similar to (porphyritic granodiorite and micro-granodiorite enclaves) or higher (all others) than the host granodiorite and show a wide range in composition (Table 4, Fig. 3).

The three gneissic enclaves analysed have low SiO_2 (52–55%) and high Al_2O_3 (23–28%), FeO_t, K_2O and MgO, indicative of a pelitic protolith. However, they do not cover the full range, which extends to quartzofeldspathic compositions. Six samples of migmatitic melanosomes (I1R, I2R) and cordierite–garnet enclaves (B25, C6, 8509, C29B) have lower SiO_2 (44–51%) and higher Al_2O_3 (>30%) than the gneissic enclaves. Four of these samples (I1R, I2R, C29B, 8509) plot in a distinct cluster (Fig. 3) characterized by high abundances of Fe, Mn, Th, Y, La and Ce, as well as moderately high Mg, Ti, V, Sc, Cr and Ni (i.e. elements controlled largely by refractory phases such as garnet, biotite, cordierite and various accessory minerals). One of the cordierite–garnet enclaves (8509) has a typical upper-crustal REE pattern similar to that of the host granodiorite (Table 5; Fig. 4), but absolute abundances, notably of the heavy rare earth elements (HREE), are considerably higher. The two subsamples (leucosome–melanosome) of migmatitic enclave I2 occupy opposite ends of the compositional range found in the metasedimentary enclaves (Fig. 3). The K- and Rb-rich nature of the leucosome is consistent with petrographic evidence for biotite melting in the migmatites.

The single quartz–cordierite enclave analysed is intermediate in Fe between the host granodiorite and the metasedimentary enclaves. Elemental concentrations are strongly controlled by the distinctive mineralogy, with high Si (quartz) and Mg (cordierite), and low abundances of alkalis and other feldspar-associated elements.

The four analysed hornfels xenoliths have highly variable compositions. Three samples have pelitic compositions but are richer in Ca than the gneissic enclaves. The fourth hornfels, sample 8503C, also has pelitic affinities but is unusually rich in Mg and Fe at the expense of feldspar-associated elements.

Among the microgranular enclaves, the porphyritic–granodioritic enclaves have compositions closest to the host granodiorite. Subtle differences include their slightly higher abundances of Fe, Ti, Th, Zr and Y, and their more variable alkali abundances. Compositions of the micro-granodioritic enclaves also resemble those of the host granodiorite. However, they are less peraluminous, Na/K ratios are higher and more variable, and abundances of Ti, Zr, Th and Y are higher, whereas those of Mg and Ni are conspicuously low. Sample F12 represents one of the granodioritic dykes, which—(on the basis of field evidence)—are believed to be related to the micro-granodioritic enclaves. The sample has slightly higher SiO_2 than the enclaves but otherwise shares their compositional characteristics.

The micro-tonalitic enclaves show substantial chemical variability, especially for Na, Ca, Mg and Ni (Fig. 3). As a group, however, they differ from the host granodiorite and the other microgranular enclave types in their higher Fe, Ca and Mg, but lower SiO_2 (56–65 %), K and Rb/Sr. REE patterns in four samples are less fractionated than those for the host granodiorite, light REE (LREE) abundances are lower, and Eu anomalies are smaller (Fig. 4). Two samples have subtle positive Eu anomalies but there is no consistent correlation between REE and other compositional characteristics. All analysed examples are peraluminous (A/CNK = 1·01–1·22).

Sm–Nd and Rb–Sr isotopes

An attempt was made to date the emplacement of the granodiorite more accurately using Rb–Sr analyses of biotite. Rather than employing the standard method of pairing the biotite with its parent rock, the biotite was leached with HCl to generate a greater dispersion in Rb/Sr and $^{87}Sr/^{86}Sr$ (Maas, in preparation). Two separate sets of unleached biotite, biotite leach and biotite residue define excellent three-point isochrons (MSWD of 0·076 and 0·043) with identical ages (425 ± 2 Ma) and initial $^{87}Sr/^{86}Sr$ [$0{\cdot}7154 \pm 3$; 95% confidence limit (CL)]. The whole rock (DR2/10) lies slightly above the mineral isochron. The whole-rock + biotite age is 422 ± 2 Ma (initial $^{87}Sr/^{86}Sr = 0{\cdot}7164 \pm 2$). Sr isotopic disequilibrium in this rock may be caused by the presence of small,

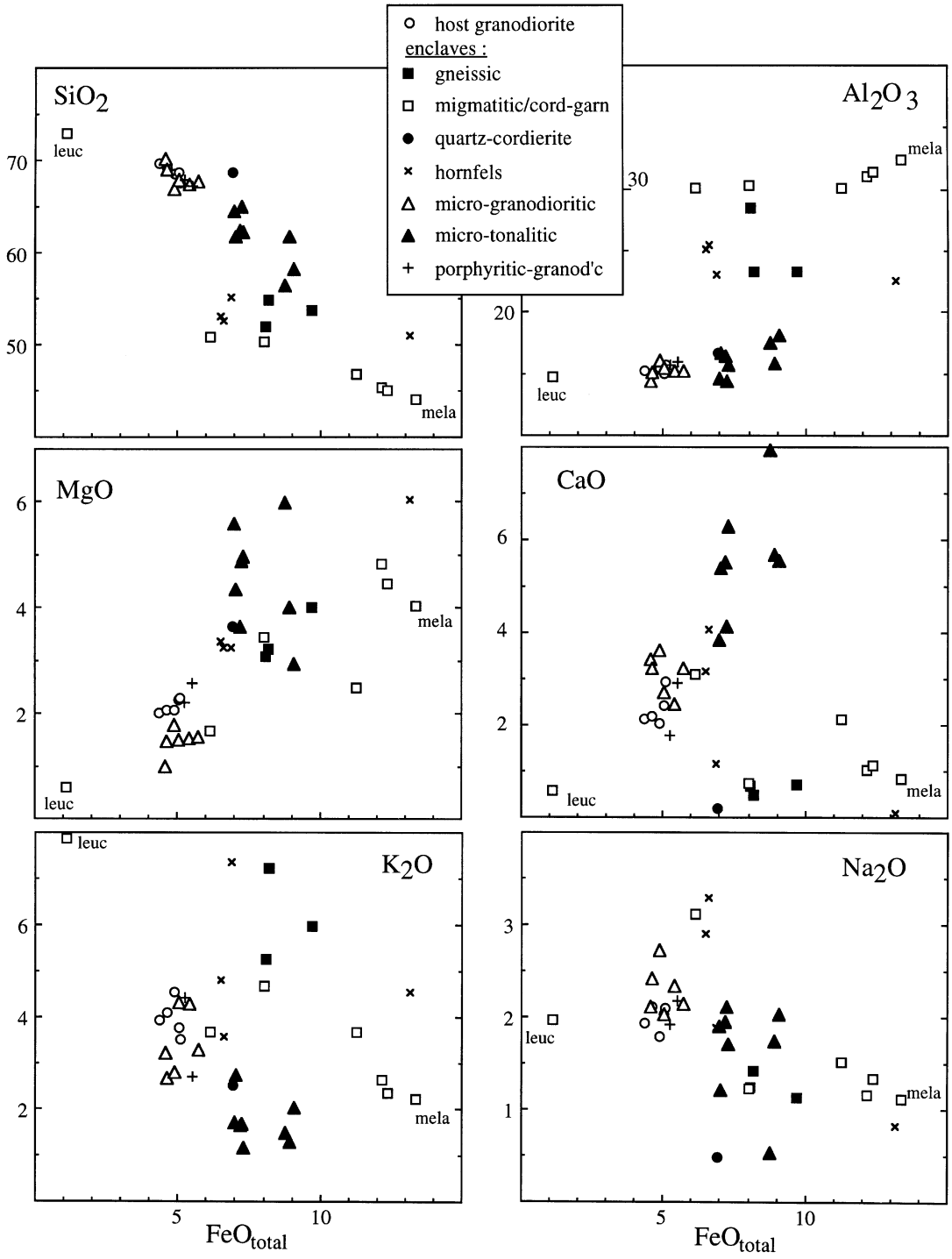
host granodiorite
enclaves :
gneissic
migmatitic/cord-garn
quartz-cordierite
hornfels
micro-granodioritic
micro-tonalitic
porphyritic-granod'c
SiO2
Al2O3
MgO
CaO
K2O
Na2O
leuc
mela
FeOtotal

Fig. 3.

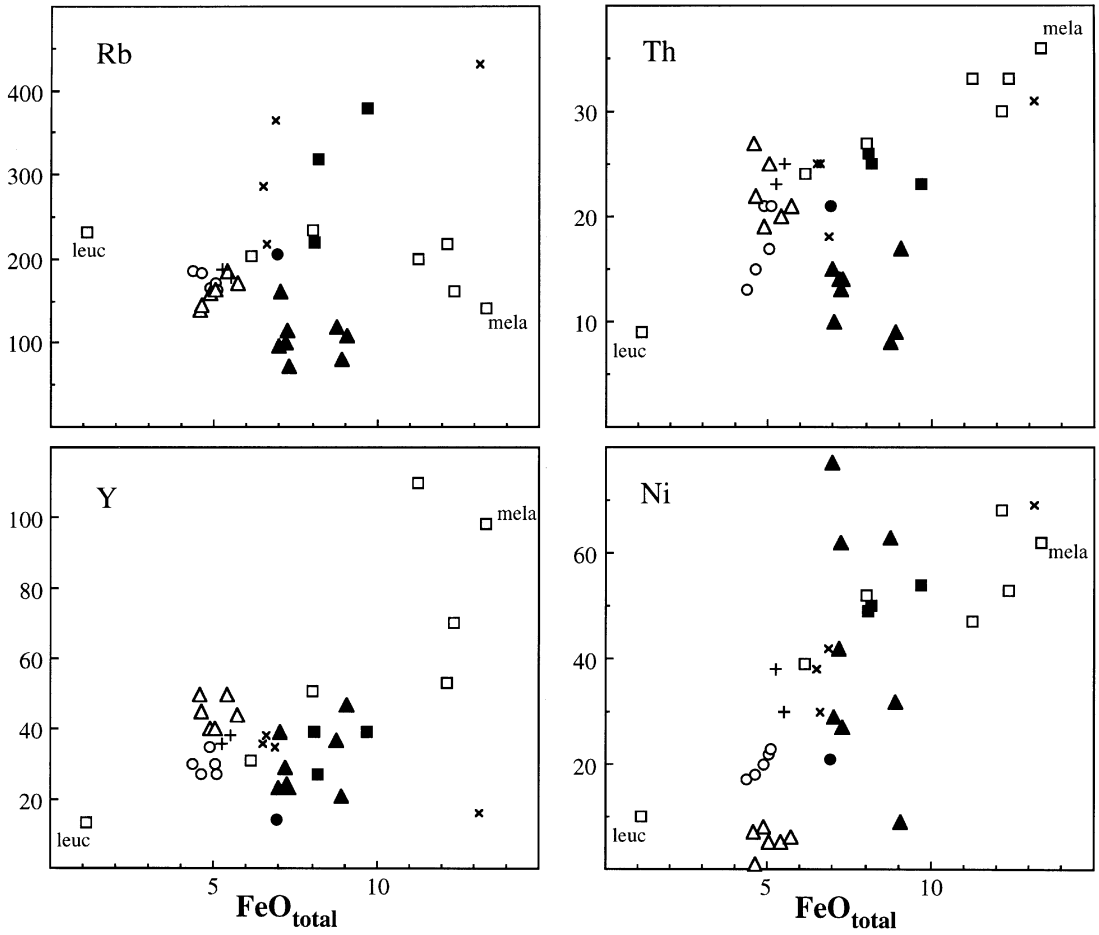

Fig. 3. Selected major and trace element abundances in the Deddick Granodiorite and its enclaves. FeO_t rather than SiO_2 is used as an index of differentiation in Harker diagrams for peraluminous compositions. leuc (leucosome) and mela (melanosome) from migmatitic enclave I2.

unequilibrated metasedimentary enclaves, which would raise the bulk $^{87}Sr/^{86}Sr$ above the ratio in the melt phase from which biotite formed. The 425 Ma biotite single-mineral isochron Rb–Sr age is considerably older than the average biotite K–Ar age of 412 Ma (Richards & Singleton, 1981), and is close to the SHRIMP U–Pb age for melt-precipitated zircon in this sample estimated from new data. We will use 425 Ma as an estimate of the age of magma emplacement.

Initial Nd and Sr isotope ratios for the Deddick Granodiorite (Table 6; Fig. 5) are close to those for other S-type plutons in the Kosciusko Batholith (McCulloch & Chappell, 1982) and indicate the influence of a mature crustal magma source. $^{87}Sr/^{86}Sr$ shows considerable scatter (0·7139–0·7162), consistent with data for other S-type granitoids (e.g. Roddick & Compston, 1977).

The high-grade metasedimentary enclaves have even higher $^{87}Sr/^{86}Sr$ and systematically lower ε_{Nd} than their host. In detail, the two gneissic enclaves analysed have higher $^{87}Sr/^{86}Sr$ than the migmatitic and cordierite–garnet enclaves (Fig. 5). This may reflect differences inherited from sedimentary protoliths, or it may be related to more advanced (Sr isotopic) equilibration of migmatitic or cordierite–garnet enclaves with the host magma. Equilibration of cordierite–garnet enclaves would be facilitated by their small size and their commonly observed partial disaggregation. However, the enclaves do not define Rb–Sr isochrons. Quartz–cordierite enclave C27B has a low ε_{Nd} value like some of the metasedimentary enclaves; however, $^{87}Sr/^{86}Sr$ cannot be determined accurately because of the high Rb/Sr ratio of the sample. The two analysed hornfels xenoliths have $^{87}Sr/^{86}Sr$ ratios similar to those of the host granodiorite but sample B29 has a lower ε_{Nd} value similar to those found for some of the high-grade metasedimentary enclaves.

Nd–Sr isotopic ratios for the microgranular enclaves show a large range, and both the micro-granodioritic and micro-tonalitic types define near-linear trends. The

Table 5: Rare earth element concentrations in the Deddick Granodiorite and selected enclaves

		Enclaves					
	host grd	m-gran	cord–garn	micro-tonalitic			
	B21	B22	8509	D1	J2	8499B	60540A
La	44·10	31·60	64·20	33·20	27·60	21·30	27·80
Ce	89·30	66·20	161·00	67·50	64·90	42·20	54·00
Pr	10·80	8·94	17·30	8·20	8·76	5·22	6·62
Nd	40·00	35·20	64·60	29·90	35·30	20·40	24·30
Sm	7·84	7·47	13·10	5·95	8·36	4·10	4·90
Eu	1·51	1·48	2·47	1·46	2·00	1·41	1·70
Gd	7·71	7·52	13·80	5·90	8·83	4·85	4·90
Tb	1·08	1·12	2·32	0·85	1·41	0·71	0·69
Dy	6·00	6·40	15·80	4·65	8·38	4·26	4·02
Ho	1·20	1·31	3·59	0·96	1·75	0·92	0·83
Er	3·22	3·62	10·10	2·62	4·80	2·66	2·45
Tm	0·49	0·55	1·53	0·40	0·69	0·43	0·37
Yb	3·13	3·59	9·93	2·70	4·50	2·96	2·52
Lu	0·47	0·52	1·40	0·40	0·69	0·45	0·39
sum REE	216·9	175·5	381·1	164·7	178·0	111·9	135·5
$(La/Sm)_n$	3·54	2·66	3·08	3·51	2·07	3·27	3·57
Eu/Eu*	0·59	0·60	0·56	0·37	0·71	0·97	1·05
$(Gd/Lu)_n$	2·05	1·80	1·22	1·84	1·59	1·33	1·56

Chondritic REE concentrations from Taylor & McLennan (1985). Eu/Eu* = 2(Eu/0·087)/[(Sm/0·231) + (Gd/0·306)]. REE measured by inductively coupled plasma mass spectrometry at Monash University. All dissolutions done in Krogh-type high-pressure vessels. Analytical uncertainties ±5% of abundance.

micro-granodioritic enclaves are consistently more primitive (higher ε_{Nd}, lower $^{87}Sr/^{86}Sr$) than the host granodiorite, in contrast to the petrographic and chemical similarities between the two rock types. The isotopic trend defined by the four analysed samples is not associated with systematic major or trace element trends, except for subtle changes in feldspar-related elements towards the levels in the host granodiorite. Despite their more mafic character, the micro-tonalitic enclaves have less primitive isotopic ratios than the micro-granodioritic enclaves. Two of the samples have isotope ratios similar to those of the metasedimentary enclaves and the host granodiorite, respectively, whereas two others have higher ε_{Nd} than the host granodiorite. Again, no consistent correlations exist between isotopic and chemical or mineralogical variation.

DISCUSSION

Gneissic, migmatitic and cordierite–garnet enclaves

A deep-seated origin for these enclaves is implied by their uniform distribution throughout the outcrop area of the host intrusion, their gneissic and migmatitic textures which distinguish them from the hornfels enclaves and low-grade metasedimentary country rocks, and *P–T* estimates (0·4–0·6 GPa, ~800°C). These enclaves originate from mid-crustal levels, within or just above the source region of the host magma. The different types of enclaves were probably derived from a range of precursors (pelitic vs psammitic), but the similarity of mineral compositions, *P–T* estimates, garnet zoning and inclusions in garnet in both gneissic and migmatitic or cordierite–garnet types suggests they formed part of the same metamorphic sequence.

Chemical windows to the mid crust

The gneissic enclaves, lacking signs of significant melting, may be used as chemical 'windows' to the mid crust (~0·4 GPa, or ~15 km) underlying the Kosciusko Batholith during the Silurian. Only the more pelitic examples of the range of pelitic to psammitic enclave compositions present have been analysed to date. Nevertheless, the three analysed gneissic enclaves resemble surmicaceous metasedimentary enclaves in the nearby Jillamatong Granodiorite (Chen *et al.*, 1989), and together they plot

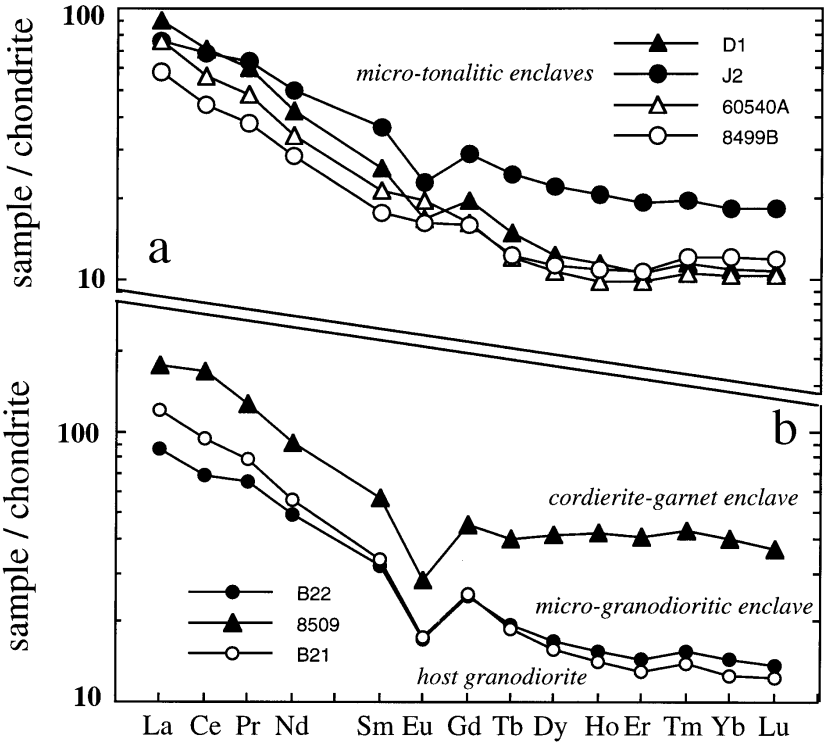

Fig. 4. Chondrite-normalized REE patterns. [Note variable Eu anomalies in the micro-tonalitic enclaves (upper panel).] High Eu/Eu* is associated with low A/CNK and high Na/K, but otherwise shows little obvious correlation with bulk enclave chemical and isotopic composition.

near the SiO_2-poor end of the compositional trends established for exposed Ordovician–Silurian sediments in this part of the Lachlan Fold Belt (Wyborn & Chappell, 1983; Munksgaard, 1988). However, Ca and Na contents in the enclaves tend to be higher than in the surface sediments at similar SiO_2 levels. ε_{Nd} and $^{87}Sr/^{86}Sr$ ratios in the Deddick enclaves are within the range observed in Cambrian to Devonian sedimentary sequences throughout the Lachlan Fold Belt (G. O'Halloran & R. Maas, in preparation). These isotopic and chemical similarities suggest that the sedimentary precursors of the enclaves may represent broad age equivalents of the Palaeozoic sediments, with chemical differences related to variations in provenance and sedimentary maturity. Using zircon age distributions, an Ordovician age has been confirmed for gneissic and cordierite–sillimanite-rich metasedimentary enclaves in the S-type Koetong Adamellite, located ~200 km to the NW in the Wagga–Omeo Metamorphic Zone (Anderson *et al.*, 1996). Confirmation of Palaeozoic mid-crust in other enclave suites would be of significance to models for the tectonic evolution (Chappell *et al.*, 1988; Gray *et al.*, 1991) and granite petrogenesis (Rossiter, 1994; Collins, 1996) in the fold belt. SHRIMP zircon studies of the Deddick gneissic enclaves are in progress to further address this problem.

Partial melting and the restite problem

With the exception of the gneissic types, partial melting evidently played a role in the evolution of most of the metasedimentary enclaves. Many have migmatitic textures with evidence for biotite breakdown to produce felsic melt. This is illustrated by the melanosome portion of metatexite enclave I2, which is rich in cordierite and contains almost no biotite. Compared with the neighbouring leucosome, it is low in SiO_2, K_2O, Ba, Rb, Sr and K/Rb, and high in Al_2O_3, MgO, MnO, FeO_t and A/CNK. Elements held largely in refractory accessories (Zr, U, Th, Y, Nb, Sc, La, Ce) are much more abundant in the melanosome, as are Ni, Cr and V. These compositional relationships are common in small-volume leucosomes (Saywer, 1996) and reflect disequilibrium melting (Bea, 1996). Disequilibium is also evident in the isotopic data: $^{87}Sr/^{86}Sr$ is higher, and ε_{Nd} is lower in the melanosome than in the leucosome.

The dominant cordierite–garnet enclaves have mineralogical and chemical characteristics similar to, and more extreme than, those of the migmatitic melanosomes and are therefore considered to represent restites from partial melting (Barbey, 1991). Because they are not associated with significant leucosome material, it is inferred that they represent metatexites which have lost melt

Table 6: Rb-Sr and Sm-Nd isotopic data for the Deddick Granodiorite and its enclaves

	Rb	Sr	$^{87}Rb/^{86}Sr$	$^{87}Sr/^{86}Sr$	Sm	Nd	$^{147}Sm/^{144}Nd$	$^{143}Nd/^{144}Nd$	$^{87}Sr/^{86}Sr(T)$	$\varepsilon_{Nd}(T)$	T_{DM}
Deddick Granodiorite											
B21	183·0	150·9	3·510	0·73622	6·87	35·22	0·1189	0·511939	0·71497	−9·7	1·96
F7	171·8	149·9	3·314	0·73399	7·08	35·98	0·1190	0·511954	0·71393	−9·4	1·94
L1	186·0	142·4	3·778	0·73707	6·46	32·03	0·1219	0·511953	0·71420	−9·5	2·00
M13	184·5	125·5	4·254	0·73975	6·33	31·14	0·1230	0·511943	0·71400	−9·8	2·05
DR2/10*	87·7	116·4	4·671	0·74458	5·79	29·41	0·1191	0·511920	0·71621	−10·0	2·00
bt 1*	139·6	16·65	24·568	0·86473	16·42	86·53	0·1147	0·511893	0·7154	−10·3	1·95
bt 1 res*	42·83	17·63	7·047	0·74831							
bt 1 lea*	310·3	14·89	62·459	1·09528							
bt 2*	146·7	18·08	23·774	0·85995							
bt 2 res*			6·976	0·75787							
bt 2 lea*			67·59	1·12655							
Metasedimentary enclaves											
Gneissic											
D6A	220·0	156·0	4·083	0·74501	9·60	52·37	0·1108	0·511856	0·72029	−10·8	1·93
G2	319·3	142·2	6·382	0·75768	9·21	47·70	0·1168	0·511861	0·71905	−11·1	2·04
Migmatite											
I2leuc	232·1	231·1	2·904	0·73546	2·51	11·72	0·1294	0·511940	0·71788	−10·2	2·21
I2mela	141·4	64·9	5·504	0·75177	14·18	78·20	0·1096	0·511832	0·71845	−11·2	1·94
Cordierite–garnet											
B25	223·8	102·1	6·353	0·75481	11·68	64·56	0·1096	0·511865	0·71635	−10·6	1·90
8509	198·9	301·6	1·909	0·72982	14·16	72·83	0·1175	0·511879	0·71826	−10·7	2·03
I1mela	161·1	94·7	4·927	0·74584	13·01	68·34	0·1150	0·511782	0·71602	−12·5	2·13
Cordierite–quartz											
C27B	204·9	14·4	42·09	0·96516	8·40	44·02	0·1154	0·511786	0·71038	−12·5	2·13
Hornfels											
B29	365·0	152·9	6·831	0·75376	9·09	47·65	0·1154	0·511934	0·71241	−9·6	1·90
B19	217·4	279·7	2·246	0·72812	10·23	57·17	0·1082	0·511757	0·71452	−12·6	2·03
Microgranitoid enclaves											
Microgranodioritic											
B22	159·9	195·6	2·362	0·72305	7·84	38·38	0·1235	0·512246	0·70875	−3·9	1·55
B22*	156·9	195·1	2·325	0·72303	7·68	37·72	0·1230	0·512244	0·70896	−3·9	
M1	146·2	197·7	2·136	0·72333	8·44	40·84	0·1249	0·512194	0·71040	−5·0	1·66
F12	140·0	119·7	3·381	0·73128	8·57	41·61	0·1245	0·512087	0·71081	−7·1	1·84
B15	183·2	127·2	4·165	0·73755	8·62	41·09	0·1268	0·512056	0·71234	−7·8	1·94
Microtonalitic											
J2	107·7	170·9	1·820	0·72402	7·82	34·46	0·1372	0·512175	0·71300	−6·0	1·97
J2*	106·3	171·0	1·801	0·72405	7·53	33·33	0·1365	0·512203	0·71315	−5·5	1·89
60540A	73·0	226·3	0·933	0·72161	4·24	20·92	0·1229	0·512013	0·71596	−8·4	1·9
D1	97·4	162·6	1·730	0·72484	5·22	25·69	0·1228	0·511963	0·71437	−9·4	2·01
8499B	114·9	184·1	1·802	0·72756	4·25	21·34	0·1205	0·511826	0·71665	−11·9	2·12

Isotope analyses (except where labelled *) were done at the Australian National University (ANU), Canberra, using procedures described by Maas & McCulloch (1991). Standards ($\pm$2 SD): SRM 987 $^{87}Sr/^{86}Sr = 0{\cdot}71020 \pm 2$, La Jolla $^{143}Nd/^{144}Nd = 0{\cdot}511875 \pm 10$, BCR-1 $^{143}Nd/^{144}Nd = 0{\cdot}512650 \pm 10$. Typical internal precisions ($2\sigma_{mean}$): $^{87}Sr/^{86}Sr < \pm 0{\cdot}00003$; $^{143}Nd/^{144}Nd < \pm 0{\cdot}000015$. Errors on $^{87}Rb/^{86}Sr$ and $^{147}Sm/^{144}Nd$ (2 SD): $\pm$0·5%, $\pm$0·2%. Definitions for $\varepsilon_{Nd}(T)$ and T_{DM} as given by DePaolo (1981). Present-day $^{143}Nd/^{144}Nd_{CHUR} = 0{\cdot}51265$, $^{147}Sm/^{144}Nd_{CHUR} = 0{\cdot}1967$. Depleted mantle model ages (T_{DM}) calculated using $^{143}Nd/^{144}Nd_{DM} = 0{\cdot}513136$ ($\varepsilon_{Nd} = 10$), $^{147}Sm/^{144}Nd_{DM} = 0{\cdot}2136$. Analyses labelled * were done at La Trobe University, adjusted to be compatible with ANU values where necessary. lea, leachate; res, residue. Initial isotope ratios calculated at 425 Ma; errors (2 SD): $\pm$0·00010 for $^{87}Sr/^{86}Sr(i)$, $\pm$0·5 units for $\varepsilon_{Nd}(T)$. Rb–Sr isochron ages calculated using ISOPLOT (Ludwig, 1991) with 2σ input errors of 0·5% for $^{87}Rb/^{86}Sr$, and 0·01% for $^{87}Sr/^{86}Sr$.

before emplacement in the host magma, or, alternatively, adhering leucosomes may have been dissolved into the host magma. It is possible that the relationship between these restitic enclaves and the host magma is genetic, i.e. they represent restite complementary to the melt component in the host magma (Chappell *et al.*, 1987), or the enclaves could be accidental restitic xenoliths. Whereas *P–T* estimates do not provide sufficient

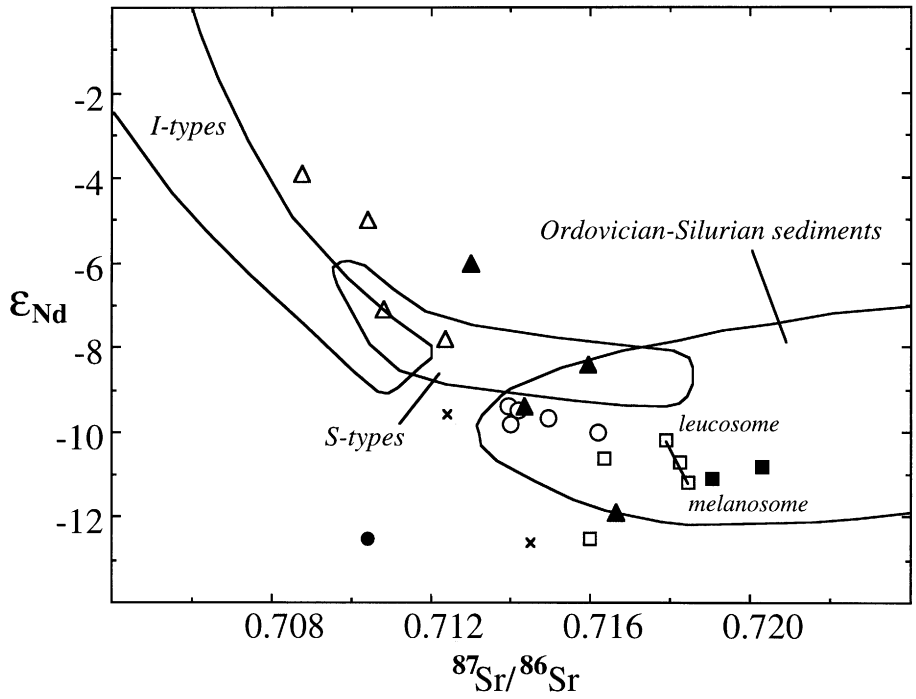

Fig. 5. Initial Nd–Sr isotope ratios for the Deddick Granodiorite and its enclaves, calculated at 425 Ma. Symbols as in Fig. 3. Leucosome and melanosome portions of migmatitic enclave I2 connected by tieline. Sr isotope ratio for the single quartz–cordierite enclave (filled circle) has a large error because of the sample's high Rb/Sr ratio. Fields for S-type and I-type granitoids in Kosciusko and Berridale Batholiths, SE Australia, shown for comparison (McCulloch & Chappell, 1982). Field for Lachlan Fold Belt Palaeozoic sediments from O'Halloran & Maas (in preparation).

resolution to rule out the first possibility, chemical and isotopic data do not support an equilibrium residue–melt relationship as implied by the simple restite unmixing model (Chappell *et al.*, 1987). Enclave bulk compositions do not fall on restite unmixing lines with the host rock (Fig. 3), and Nd–Sr isotopic compositions of the enclaves differ significantly from those of the host. Enclave plagioclase has a maximum anorthite content of 40 mol %, whereas the plagioclase cores in the host [considered to be part of the melt-complementary restite (Chappell *et al.*, 1987)] are relatively uniform around 50 mol % anorthite. Biotite and cordierite compositions in the enclaves are significantly less magnesian than their magmatic counterparts in the host magma, and therefore also inconsistent with a simple restite–melt relationship.

Lack of chemical complementarity between enclaves and host, and mineral compositional disequilibria of the type described here have also been observed in other studies (Price, 1983; Chen *et al.*, 1989; Montel *et al.*, 1991). It was suggested that such enclaves were derived from refractory parts of the magma source where melting was insufficient to disrupt the metamorphic fabric of the rocks. Consequently, these lithologies would not be able to influence the magma composition in the form of melt and dispersed restite crystals and would be preserved as enclaves (Chen *et al.*, 1989). This interpretation cannot be applicable to the precursors of the restitic Deddick enclaves, which have undergone extensive partial melting. Rather, if the enclave precursors did form part of the magma source, the chemical and isotopic disequilibria suggest that this material represents only part of a spectrum of source materials. The magma source must have also included more Ca–Na-rich components with lower $^{87}Sr/^{86}Sr$ and higher ε_{Nd}, such as feldspathic metasedimentary rocks, or a mafic magma may have mixed with metasediment-derived magma to form the host magma. It should be reiterated in this context that crustal melting in isotopically heterogeneous protoliths need not lead to establishment of isotopic equilibrium. When melting and melt segregation are rapid relative to diffusive re-equilibration, melt may escape with isotopic (e.g. Sr, Pb) and chemical features not representative of the protolith (Hogan & Sinha, 1991; Barbero *et al.*, 1995; Pichavant *et al.*, 1996). The possibility exists, therefore, that the metasedimentary enclaves represent a major source component of the host magma, despite the observed Sr isotopic variations. However, this is not supported by the Nd isotopic and bulk chemical data.

If the metasedimentary enclaves are in fact accidental xenoliths, their restitic and migmatitic features may have

formed during prolonged residence in the host (>800°C) magma, or they may be relicts from an older melting event. The first alternative cannot account for the fold structures in the migmatitic enclaves, which must predate entrapment in the host magma. The second alternative can be tested by precise U–Pb dating of leucosome formation, and this is currently the subject of SHRIMP U–Pb studies of the enclaves.

Whatever their origin, the cordierite–garnet enclaves clearly contributed material to the host magma in the form of garnet and (sillimanite-bearing) cordierite xenocrysts derived from the mechanical disaggregation of their parent enclaves, and perhaps also in the form of resorbed leucosomes. Based on the modal abundance of cordierite in the host granodiorite (Legg, 1988), this contribution may account for ~5 vol. % of the host phase, but its effect on the budget of certain trace elements may be greater if accessory mineral grains were transferred along with garnet and cordierite. Not unexpectedly, cordierite xenocrysts appear to have been chemically adjusted in the host magma (see Table 1), whereas xenocrystic garnet grains have reaction rims or are overgrown by magmatic garnet but otherwise resisted re-equilibration. Mineral grains of this type could be considered typical restite (Chappell *et al.*, 1987), yet our results suggest they are derived from rocks that were xenoliths or, at the very most, represent only part of the crustal magma source. This illustrates the problems inherent in attempting to recognize material which is truly restitic relative to its magmatic host (Wall *et al.*, 1987; Brown *et al.*, 1995).

Microgranular enclaves

Micro-granodioritic enclaves

These enclaves appear to be related to compositionally similar granitoid dykes. Field evidence suggests that the dykes were emplaced into incompletely solidified host magma, and that near-solid dyke material was disrupted during late movement of the highly crystalline host (Fernandez & Barbarin, 1991). Dyke disruption in a highly crystalline host magma can explain the large size (>50 cm) and sharp angular outlines of these enclaves (Pitcher, 1991), and the limited extent of physical interaction with the host magma (Barbarin, 1991). Igneous microstructures throughout the enclaves support a magmatic origin. However, despite chemical similarities to the host rock (Figs 3 and 4), a cognate origin is ruled out by the pronounced isotopic contrast (Fig. 5), the lower Mg–Ni and higher Ti contents in the enclaves at comparable FeO_t and SiO_2 levels, and differing compositions of primary biotite.

Isotopic disequilibrium in pluton-hosted microgranular enclaves is rarely as pronounced and consistent as in the Deddick enclaves (e.g. Eberz *et al.*, 1990; Metcalf *et al.*, 1995; Moreno-Ventas *et al.*, 1995); in many examples, enclaves and host have similar Sr-isotope (e.g. Holden *et al.*, 1987) and often also Nd-isotope ratios (Pin *et al.*, 1990; Fourcade & Javoy, 1991), regardless of enclave bulk compositions. This is generally thought to reflect rapid diffusive isotopic equilibration following entrainment (e.g. Fourcade & Javoy, 1991) rather than a primary feature (Chen *et al.*, 1990). The Rb–Sr system is frequently more thoroughly equilibrated than the Sm–Nd system (e.g. Holden *et al.*, 1991). Rapid diffusive isotopic exchange, and the greater resilience of the Sm–Nd system, have been substantiated by diffusion experiments using isotopically distinct mafic and felsic compositions (Baker, 1989; Lesher, 1990, 1994).

By contrast, the coherent Sr–Nd isotope variation shown by the three analysed Deddick enclaves and one sample (F12) of a related granitoid dyke indicates that differential diffusive isotopic exchange was not important, presumably because both dyke and host magma had largely solidified before enclave formation. The isotope data indicate that the source of the enclave magma differed from that of the host magma, at least in age. The most primitive isotopic composition (for sample B22) is the closest estimate for this source. Isotopic variability within this enclave population probably tracks the progressive contamination of a homogeneous enclave parent magma with crustal material, presumably through magma mixing at depth (Barbarin & Didier, 1992), or through variable local mixing within individual dykes (Pitcher, 1991; Fernandez & Barbarin, 1991). For example, bulk mixing between an enclave magma (represented, e.g. by enclave B22) and another magma with similar Sr/Nd ratio (e.g. the host magma), could produce the near-linear Nd–Sr isotope trend defined by the enclaves. Petrographic evidence for mixing exists in the form of garnet xenocrysts, and mixing could also explain disequilibrium between orthopyroxene and biotite in these enclaves. However, unlike their isotopic ratios, bulk chemical compositions of the enclaves resemble those of the host rock and show little systematic variation (Figs 3 and 4), presumably because pre-mixing end-member compositions were already similar. Exceptions are Ca, Na, Sr and Na/K which decrease, and K and Rb/Sr which increase towards the levels in the host as $^{87}Sr/^{86}Sr$ increases, consistent with bulk mixing. Other elements, such as Mg, Ni, Ti or Th, remain at levels that are subtly but consistently different from those in the host. This suggests buffering of ferromagnesian elements (and high field strength elements) by a small degree of crystallization during mixing.

The origin of the dyke–enclave magma is unclear. The present mineralogy (with primary orthopyroxene) and

chemistry of the enclaves are common in S-type granitoids of the Kosciusko Batholith S-types (Hine *et al.*, 1978) but the evidence reviewed above indicates that these characteristics were acquired through contamination of a magma that was isotopically, but not necessarily chemically, primitive relative to the Kosciusko Batholith S-types. Isotopic compositions like those in the least contaminated enclave B22 are found for some other S-types, e.g. in the Dalgety Granodiorite 70 km to the NNE (McCulloch & Chappell, 1982), and S-types in central Victoria have even higher ε_{Nd} and lower $^{87}Sr/^{86}Sr$ (Elburg & Nicholls, 1995; Elburg, 1996*b*). Some I-type granites in the Kosciusko Batholith [e.g. the Jindabyne Tonalite (McCulloch & Chappell, 1982)] are also isotopically similar. The original dyke–enclave magma could therefore have been derived from an I-type or from another S-type magma, followed by contamination during ascent through, and interaction with, the host magma.

Micro-tonalitic enclaves

Following Didier (1973, 1987), these enclaves are readily classified as mafic microgranular enclaves. The origin of such enclaves is controversial (hybrid magma globule, cognate, restite) but there is good evidence here not only for an igneous origin, but also for the commingled hybrid magma globule model. This evidence includes igneous microstructures throughout the enclaves, highly magnesian and calcic compositions in phenocryst and groundmass mafic phases and feldspars, respectively, the presence of (rare) phenocryst assemblages that are similar to those of andesitic rocks, and the occurrence of mineral and isotopic disequilibria typical of magma mixing. For example, clots of orthopyroxene euhedra with highly magnesian, bronzitic (Mg_{80}) cores occur in one enclave, whereas orthopyroxene phenocrysts and groundmass crystals in the range $Mg_{79–51}$ are common in other enclaves. Another enclave contains a small aggregate comprising euhedral hypersthene mantled by Ca-clinopyroxene. Small plagioclase laths in the groundmass are anorthite rich ($An_{79–51}$), as is the plagioclase ($An_{85–80}$) which overgrows plagioclase xenocrysts.

The bronzitic orthopyroxene cores rule out a cognate origin for these enclaves. Crystallization experiments have established that hypersthene (never $>Mg_{55}$) rather than bronzite is the typical near-liquidus orthopyroxene in acid–intermediate liquids (Clemens & Wall, 1981; Conrad *et al.*, 1988). Bronzite could not have formed if the original granitic magma was peraluminous, as could be inferred from the measured bulk chemistry of the enclaves. Moreover, the presence of igneous hypersthene–clinopyroxene aggregates, the bronzite cores and the observed textures are difficult to reconcile with a restitic origin or derivation from refractory source lithologies, even if these contained a small amount of trapped granitic melt (Chen *et al.*, 1989). On the other hand, bronzite-phyric, clinopyroxene-free high-Mg andesites have been reported from Japan (Tatsumi & Ishizaka, 1982), and clinopyroxene–orthopyroxene aggregates are common in many natural and experimental andesitic assemblages. We therefore interpret the pyroxenes and the calcic plagioclase to have formed in a melt that was andesitic in composition, and probably unusually magnesian for such an intermediate composition.

Other mineralogical observations indicate that magma mixing was involved in producing the enclave magma(s). The most conspicuous of these are the xenocrysts of plagioclase and cordierite, which appear to have been derived from the host magma and are associated with overgrowths that are in equilibrium with a more mafic (more Mg–Ca-rich) melt. Garnet and quartz (quartz ocelli) xenocrysts were also derived from the host magma. Late interstitial quartz pools are crowded with acicular apatite. All of these observations are typical of systems for which other evidence for magma mingling–mixing is strong (Didier, 1973; Vernon, 1984, 1990). The wide range in the compositions of biotite ($Mg_{65–51}$) and other minerals also illustrates the unequilibrated mineralogy of the enclaves. We conclude that the enclave magma(s) formed from basaltic or andesitic magma which underwent incomplete mixing with the more felsic Deddick host magma.

Chemically these enclaves differ strongly from the host granodiorite (Fig. 3). Major element compositions in some samples have andesitic affinities (Table 4), and data for several elements (e.g. Ca, Si, K, Mg, Rb, Ba) plot roughly between the fields of the host granodiorite and common basaltic–andesitic compositions, as would be expected if simple bulk mixing was important. Most trace elements track the distributions in the host rock, but at a lower overall level, e.g. on a mid-ocean ridge basalt (MORB) normalized spidergram (not shown). Again, this is an expected result given the evidence for crystal transfer from the host magma and indirectly from disintegrated, trace-element-rich metasedimentary enclaves. REE patterns are also similar to those in the host rock but some features of the original more mafic magma remain, such as lower total REE and high Eu/Eu* (Fig. 5). Finally, Sr–Nd isotopic data form an extensive array consistent with bulk mixing. It is noted, however, that trends for most elements are scattered and data for some elements (e.g. Na, Al, Ti, Ni, Cr) do not support simple mixing alone. Furthermore, the isotopic variations are not consistently correlated with other chemical changes. Inconsistencies of this type are common in mafic microgranular enclaves and are variously ascribed to the influence of more complex magmatic processes (Koyaguchi, 1986; Poli & Tommasini, 1991), interdiffusion (Debon, 1991) or combinations of these (Eberz & Nicholls, 1990). Some of these processes are inferred to have been

involved in the evolution of the Deddick enclaves. First, magma mixing of an inferred basaltic–andesitic magma with a more felsic host magma would have been possible only after a considerable reduction in the rheological contrast between the two magmas. Depending on the mass fraction of the more mafic magma (Poli *et al.*, 1996), this would require a degree of crystallization and/or diffusive equilibration in the more mafic magma, which would produce a spectrum of hybrid magmas available for mixing. This could explain part of the scatter in the enclave compositions. Second, the felsic host magma was probably not homogeneous. This is evident from the Nd–Sr isotope data, which extend beyond the ratios of the host rock (Fig. 5), indicating that material derived from the metasedimentary enclaves was an additional important mixing component. Third, evidence for pervasive diffusive alteration exists in the form of zoned enclaves with biotite-free cores rich in orthopyroxene and secondary actinolite presumably after Ca-clinopyroxene, and distinct biotite-bearing rims. Both heterogeneous mixing and diffusive chemical exchange therefore contributed to the compositional scatter (see also Barbarin & Didier, 1992).

Despite such complications, the micro-tonalitic enclaves can be clearly identified as the products of arrested hybridization of a commingled, more mafic magma of basaltic or andesitic composition. However, the trace element and isotopic signatures of this magma have largely been obscured, complicating comparison with the (rare) mafic complexes in the area, such as the Blind Gabbro (Hine *et al.*, 1978). It is noted that very similar microgranular enclaves have been described from the peraluminous Cowra Granodiorite in central New South Wales (Wyborn *et al.*, 1991). Like their Deddick counterparts, the Cowra enclaves contain quartz ocelli (Vernon, 1983), high-Mg orthopyroxene cores, acicular apatite and calcic plagioclase (up to An_{90}). Some samples have positive Eu anomalies. Wyborn *et al.* (1991) dismissed an igneous (basaltic–andesitic) origin for these enclaves because they are weakly peraluminous and comparatively low in Na, and interpreted the enclaves as residues from partial melting of metasedimentary protoliths. Similarly, White *et al.* (1991) claimed that most microgranular enclaves in SE Australian S-type granitoids represent metamorphic rock fragments from granite source regions. Based on our observations in the Deddick Granodiorite, we disagree with these interpretations and concur with Vernon (1983), who suggested that the Cowra enclaves represent frozen globules of a more mafic magma that had undergone mixing with the more felsic host magma. Recent studies of microgranular enclaves in other S-type granitoids and volcanics from the Lachlan Fold Belt in Victoria have reached similar conclusions (Elburg & Nicholls, 1995; Elburg, 1996*a*,*b*).

Porphyritic granodioritic enclaves

This group of enclaves is most readily interpreted as representing fragments eroded from a marginal facies of the host granodiorite, i.e. these are cognate enclaves [the 'felsic microgranular enclaves' of Didier (1973)]. This is supported by close mineralogical and chemical affinities with the host, porphyritic textures and higher modal abundances of the same mafic phases that occur in the host, and by the presence of similar material as rinds on hornfels xenoliths in marginal parts of the pluton. The similarities between this rapidly crystallized material and its host rock suggest that the host magma underwent little differentiation after emplacement, consistent with the consistently mafic nature of the granodiorite.

Pluton-scale mixing in the host granodiorite?

The interpretation of microgranular enclaves as commingled mafic magma globules implies that mafic magma(s) acted not only as a heat source to induce crustal melting, but that some mafic magma mixed with crustally derived granitic magma to form hybrid peraluminous magma. The important question is then the extent of hybridization, i.e. is the process efficient enough to form large, pluton-size batches of magma? Evidence for large-scale hybridization as the dominant process has been reported for some zoned, metaluminous intrusions where gabbroic and intermediate compositions are present (e.g. Reid & Hamilton, 1987; Metcalf *et al.*, 1995), and the concept has also been applied to peraluminous complexes (Bussy, 1991; Clarke & Chatterjee, 1991; Castro *et al.*, 1991; Moreno-Ventas *et al.*, 1995). The key evidence cited is usually the association of heterogeneous granitoids, mafic stocks, large numbers of mafic microgranular enclaves, and hyperbolic Nd–Sr isotope (mixing) trends.

In the Deddick Granodiorite, hybrid igneous enclaves are present, and together with the metasedimentary enclaves they form an extensive Nd–Sr array centred on the host, which itself shows a degree of isotopic heterogeneity (Fig. 5). This trend could be generated by magma mixing or assimilation of metasediment by basaltic melt (represented in modified form by hybrid enclaves). Evidence of another form of magma contamination, conceivably with similar isotopic effects, is preserved as up to 5 vol. % of dispersed xenocrysts derived from disintegrated residual metasedimentary enclaves. However, bulk compositions of the host granodiorite are comparatively homogeneous and cannot readily be accommodated within a pluton-scale mixing model using the enclave compositions as end members. A number of reasons could account for this observation. Convective blending may have erased any hybrid zones in the

host magma, whereas hybridization is incomplete, and therefore detectable, only in the small volumes of isotopically distinct magma preserved as microgranular enclaves. At the same time, enclave compositions may be too strongly modified by interdiffusion to provide useful mixing constraints. On the other hand, it is equally possible that the proportion of mafic magma was simply too small to noticeably affect the composition of the felsic host magma. This is supported by the small proportion of micro-tonalitic enclaves ($\ll 1$ vol.%) observed at the level exposed at present. By contrast, resolvable chemical variations owing to incomplete hybridization are preserved in the host phase of the I-type Swifts Creek Pluton (Central Victoria), where enclaves form up to 40% of the outcrop (Eberz *et al.*, 1990). However, the common (almost ubiquitous) occurrence of mafic microgranular enclaves in many S-type granitoids, and the isotopic heterogeneity of the granites on a regional scale, suggests that interaction of basaltic–andesitic magmas with crustal magmas is of some, or possibly major, importance in S-type petrogenesis in general.

ACKNOWLEDGEMENTS

A significant portion of this paper is based on the results of Colin Legg's B.Sc. (Honours) thesis from 1988. Unfortunately, Colin was not available to publish his own work. Many of his ideas have been incorporated into this paper but the final conclusions differ and are the responsibility of the other authors. We thank Dr M.T. McCulloch for permission to use the mass spectrometric facilities at the Australian National University, Canberra.

REFERENCES

Anderson, J. A. C., Williams, I. S., Price, R. C. & Fleming, P. D., 1996. U–Pb zircon ages from NE Victoria, implications for granite genesis and the local basement. *10th Annual Victorian Universities Conference, University of Melbourne, Abstracts*. Melbourne: University of Melbourne, pp. 21–22.

Baker, D. R., 1989. Tracer versus trace element diffusion: diffusional decoupling of Sr concentration from Sr isotope composition. *Geochimica et Cosmochimica Acta* **53,** 3015–3023.

Barbarin, B., 1991. Enclaves of the Mesozoic calc-alkaline granitoids of the Sierra Nevada Batholith, California. In: Didier, J. & Barbarin, B. (eds) *Enclaves and Granite Petrology*. Amsterdam: Elsevier, pp. 135–153.

Barbarin, B. & Didier, J., 1992. Genesis and evolution of mafic microgranular enclaves through various types of interaction between coexisting felsic and mafic magmas. *Transactions of the Royal Society of Edinburgh* **83,** 145–154.

Barbero, L., Villaseca, C., Rogers, G. & Brown, P. E., 1995. Geochemical and isotopic disequilibrium in crustal melting: an insight from the anatectic granitoids from Toledo, Spain. *Journal of Geophysical Research* **100,** 15745–15765.

Barbey, P., 1991. Restites in migmatites and autochthonous granites: their main features and their genesis. In: Didier, J. & Barbarin, B. (eds) *Enclaves and Granite Petrology*. Amsterdam: Elsevier, pp. 479–492.

Bea, F., 1996. Controls on trace element composition of crustal melts. *Transactions of the Royal Society of Edinburgh, Earth Sciences* **87,** 33–41.

Berman, R. G., 1990. Mixing properties of Ca–Mg–Fe–Mn garnets. *American Mineralogist* **75,** 328–344.

Bohlen, S. R., Wall, V. J. & Boettcher, A. L., 1983. Experimental investigation and application of equilibria in the system FeO–TiO_2–Al_2O_3–SiO_2–H_2O. *American Mineralogist* **68,** 1049–1058.

Brown, M., Rushmer, T. & Sawyer, E. W., 1995. Introduction to special section: mechanisms and consequences of melt segregation from crustal protoliths. *Journal of Geophysical Research* **100,** 15551–15563.

Bussy, F., 1991. Enclaves of the Late Miocene Monte Capanne granite, Elba Island, Italy. In: Didier, J. & Barbarin, B. (eds) *Enclaves and Granite Petrology*. Amsterdam: Elsevier, pp. 167–178.

Castro, A., Moreno-Ventas, I. & de la Rosa, J., 1991. H-type (hybrid) granitoids: a proposed revision of the granite-type classification and nomenclature. *Earth-Science Reviews* **31,** 237–253.

Chappell, B. W. & White, A. J. R., 1992. I- and S-type granites in the Lachlan Fold Belt. *Transactions of the Royal Society of Edinburgh, Earth Sciences* **83,** 1–26.

Chappell, B. W., White, A. J. R. & Wyborn, D., 1987. The importance of residual source material (restite) in granite petrogenesis. *Journal of Petrology* **28,** 1111–1138.

Chappell, B. W., White, A. J. R. & Hine, R., 1988. Granite provinces and basement terranes in the Lachlan Fold Belt, SE Australia. *Australian Journal of Earth Sciences* **35,** 505–521.

Chappell, B. W., White, A. J. R. & Williams, I. S., 1991. A transverse section through granites of the Lachlan Fold Belt. *Excursion Guide, 2nd Hutton Symposium, Canberra 1991*. Canberra: Bureau of Mineral Resources.

Chen, Y. D., Price, R. C. & White, A. J. R., 1989. Inclusions in three S-type granites from SE Australia. *Journal of Petrology* **30,** 1181–1218.

Chen, Y. D., Price, R. C., White, A. J. R. & Chappell, B. W., 1990. Mafic inclusions from the Blue Gum and Glenbog granite suites, SE Australia. *Journal of Geophysical Research* **95,** 17757–17785.

Clarke, D. B. & Chatterjee, A. K., 1991. The Liscomb Complex: a microcosm of peraluminous granite production in the Meguma Zone of Nova Scotia. *2nd Hutton Symposium, Canberra, Abstracts*. Canberra: Bureau of Mineral Resources, p. 26.

Clemens, J. D., 1981. The origin and evolution of some peraluminous acid magmas (experimental, geochemical and petrological investigations). Ph.D. Thesis, Monash University, Melbourne, Vic.

Clemens, J. D., 1988. Volume and composition relationships between granites and their lower crustal source regions: an example from central Victoria, Australia. *Australian Jounal of Earth Sciences* **35,** 445–449.

Clemens, J. D. & Vielzeuf, D., 1987. Constraints on melting and magma production in the crust. *Earth and Planetary Science Letters* **86,** 287–306.

Clemens, J. D. & Wall, V. J., 1981. Crystallization and origin of some peraluminous (S-type) granitic magmas. *Canadian Mineralogist* **19,** 111–132.

Clemens, J. D. & Wall, V. J., 1984. Origin and evolution of a peraluminous silicic ignimbrite suite: the Violet Town Volcanics. *Contributions to Mineralogy and Petrology* **88,** 354–371.

Collins, W. J., 1996. Lachlan Fold Belt granitoids: products of three-component mixing. *Transactions of the Royal Society of Edinburgh, Earth Sciences* **87,** 171–181.

Conrad, W. K., Nicholls, I. A. & Wall, V. J., 1988. Water-saturated and -undersaturated melting of metaluminous and peraluminous

crustal compositions at 10 kb: evidence for the origin of silicic magmas in the Taupo Volcanic Zone, and other occurrences. *Journal of Petrology* **29,** 765–803.

Debon, F., 1991. Comparative major element chemistry in various 'microgranular enclave–plutonic host' pairs. In: Didier, J. & Barbarin, B. (eds) *Enclaves and Granite Petrology.* Amsterdam: Elsevier, pp. 293–312.

DePaolo, D. J., 1981. A neodymium and strontium isotope study of the Mesozoic calc-alkaline granitic batholiths of the Sierra Nevada and Peninsular Ranges, California. *Journal of Geophysical Research* **86,** 10470–10501.

Didier, J., 1973. *Granites and their Enclaves. The Bearing of Enclaves on the Origin of Granites.* Amsterdam: Elsevier, 393 pp.

Didier, J., 1987. Contribution of enclave studies to the understanding of origin and evolution of granitic magmas. *Geologische Rundschau* **76,** 41–50.

Didier, J. & Barbarin, B. (eds), 1991. *Enclaves and Granite Petrology.* Amsterdam: Elsevier, 625 pp.

Eberz, G. W. & Nicholls, I. A., 1990. Chemical modification of enclave magma by post-emplacement crystal fractionation, diffusion and metasomatism. *Contributions to Mineralogy and Petrology* **104,** 47–55.

Eberz, G. W., Nicholls, I. A., Maas, R., McCulloch, M. T. & Whitford, D. J., 1990. The Nd- and Sr-isotopic composition of I-type microgranular enclaves and their host rocks from the Swifts Creek Pluton, southeast Australia. *Chemical Geology* **85,** 119–134.

Elburg, M. A., 1996*a*. Evidence of isotopic equilibration between microgranitoid enclaves and host granodiorite, Warburton Granodiorite, Lachlan Fold Belt, Australia. *Lithos* **38,** 1–22.

Elburg, M. A., 1996*b*. Three types of enclaves in a peraluminous ignimbrite suite, Violet Town Volcanics, SE Australia: constraints on their origin and evolution. *Journal of Petrology.* **37,** 1385–1408.

Elburg, M. A. & Nicholls, I. A., 1995. Origin of microgranitoid enclaves in the S-type Wilson's Promontory Batholith, Victoria: evidence for magma mingling. *Australian Journal of Earth Sciences* **42,** 423–435.

Feldstein, S. N., Halliday, A. N., Davies, G. R. & Hall, C. M., 1994. Isotope and chemical microsampling: constraints on the history of an S-type rhyolite, San Vincenzo, Italy. *Geochimica et Cosmochimica Acta* **58,** 943–958.

Fernandez, A. N. & Barbarin, B., 1991. Relative rheology of coeval mafic and felsic magmas: nature of resulting interaction processes and shape and mineral fabrics of mafic microgranular enclaves. In: Didier, J. & Barbarin, B. (eds) *Enclaves and Granite Petrology.* Amsterdam: Elsevier, pp. 263–275.

Ferry, J. M. & Spear, F. S., 1978. Experimental calibration of the partitioning of Fe and Mg between biotite and garnet. *Contributions to Mineralogy and Petrology* **66,** 113–117.

Fleming, P. D., 1991. Structures in metasedimentary inclusions as 'windows' into granite source regions. *2nd Hutton Symposium, Canberra, Abstracts.* Canberra: Bureau of Mineral Resources, p. 36.

Fourcade, S. & Javoy, M., 1991. Sr–Nd–O isotopic features of mafic microgranular enclaves and host granitoids from the Pyreneees, France: evidence for their hybrid nature and inference on their origin. In: Didier, J. & Barbarin, B. (eds) *Enclaves and Granite Petrology.* Amsterdam: Elsevier, pp. 345–364.

Ganguly, J. & Saxena, S. K., 1984. Mixing properties of aluminosilicate garnets: constraints from natural and experimental data and applications to geothermobarometry. *American Mineralogist* **69,** 88–97.

Glen, R. A., 1992. Thrust, extensional and strike-slip tectonics in an evolving Paleozoic orogen—a structural synthesis of the Lachlan Orogen of SE Australia. *Tectonophysics* **214,** 341–380.

Glen, R. A. & Vandenberg, A. H. M., 1987. Thin-skinned tectonics in part of the Lachlan Fold belt near Delegate, SE Australia. *Geology* **15,** 1070–1073.

Gray, D. R., 1988. Structure and tectonics. In: Douglas, J. G. & Ferguson, J. A. (eds) *Geology of Victoria.* Melbourne: Geological Society of Australia, Victorian Division, pp. 1–36.

Gray, D. R., Wilson, C. J. L. & Barton, T. J., 1991. Intracrustal detachments and implications for crustal evolution within the Lachlan Fold Belt, SE Australia. *Geology* **19,** 574–577.

Harley, S. L., 1984. An experimental study of the partitioning of Fe and Mg between garnet and orthopyroxene. *Contributions to Mineralogy and Petrology* **86,** 359–373.

Hine, R., Williams, I. S., Chappell, B. W. & White, A. J. R., 1978. Contrasts between I- and S-type granitoids of the Kosciusco Batholith. *Journal of the Geological Society of Australia* **25,** 219–234.

Hodges, K. V. & Crowley, P. D., 1985. Error estimations and empirical geothermobarometry for pelitic systems. *American Mineralogist* **70,** 702–709.

Hodges, K. V. & Spear, F. S., 1982. Geothermometry, geobarometry and the Al_2SiO_5 triple point at Mt. Moosilauke, New Hampshire. *American Mineralogist* **67,** 1118–1134.

Hoffer, E. & Grant, J. A., 1980. Experimental investigation of the formation of cordierite–orthopyroxene parageneses in pelitic rocks. *Contributions to Mineralogy and Petrology* **73,** 15–22.

Hogan, J. P. & Sinha, A. K., 1991. The effect of accessory minerals on the redistribution of lead isotopes during crustal anatexis: a model. *Geochimica et Cosmochimica Acta* **55,** 335–348.

Holdaway, M. J., 1971. Stability of andalusite and the aluminum silicate phase diagram. *American Journal of Science* **271,** 97–131.

Holden, P., Halliday, A. N. & Stephens, W. E., 1987. Nd and Sr isotope content of microdiorite enclaves point to mantle input to granite production. *Nature* **330,** 53–56.

Holden, P., Halliday, A. N., Stephens, W. E. & Henny, P. J., 1991. Chemical and isotopic evidence for mass transfer between mafic enclaves and felsic magma. *Chemical Geology* **92,** 135–152.

Indares, A. & Martignole, J., 1985. Biotite–garnet geothermometry in the granulite facies: the influence of Ti and Al in biotite. *American Mineralogist* **70,** 272–278.

Juteau, M., Michard, A. & Albarede, F., 1986. The Pb–Sr–Nd isotope geochemistry of some recent circum-Mediterranean granites. *Contributions to Mineralogy and Petrology* **92,** 331–340.

Koyaguchi, T., 1986. Evidence for two-stage mixing in magmatic inclusions and rhyolitic lava domes on Niijima Island, Japan. *Journal of Volcanological and Geothermal Research* **29,** 71–98.

Kozial, A. M., 1989. Recalibration of the garnet–plagioclase–Al_2SiO_5–quartz (GASP) geobarometer and applications to natural parageneses. *EOS* **70,** 493.

Lee, D. E. & Christiansen, E. H., 1983. The granite problem as exposed in the Southern Snake Range, Nevada. *Contributions to Mineralogy and Petrology* **83,** 99–116.

Lee, H. Y. & Ganguly, J., 1988. Equilibrium compositions of coexisting garnet and orthopyroxene: experimental determinations in the system FeO–MgO–Al_2O_3–SiO_2 and applications. *Journal of Petrology* **29,** 93–114.

Legg, C., 1988. Geology and geochemistry of the Deddick Granodiorite, NE Victoria. B.Sc. (Hons.) Thesis, Monash University, Melbourne, Vic.

Lesher, C. E., 1990. Decoupling of chemical and isotopic exchange during magma mixing. *Nature* **344,** 235–237.

Lesher, C. E., 1994. Kinetics of Sr and Nd exchange in silicate liquids: theory, experiments, and applications to uphill diffusion, isotopic equilibration, and irreversible mixing of magmas. *Journal of Geophysical Research* **99,** 9585–9604.

Ludwig, K. R., 1991. ISOPLOT for MS-DOS, a plotting and regression program for radiogenic isotope data: revision of USGS Open-File Report 88-557. Denver, CO: US Geological Survey.

Maas, R. & McCulloch, M. T., 1991. The provenance of Archean clastic metasediments in the Narryer Gneiss Complex, Western Australia: trace element geochemistry, Nd isotopes, and U–Pb ages for detrital zircons. *Geochimica et Cosmochimica Acta* **55,** 1915–1932.

Maury, R. C. & Didier, J., 1991. Xenoliths and the role of assimilation. In: Didier, J. & Barbarin, B. (eds) *Enclaves and Granite Petrology.* Amsterdam: Elsevier, pp. 529–542.

McCulloch, M. T. & Chappell, B. W., 1982. Nd and Sr isotopic characteristics of S- and I-type granites. *Earth and Planetary Science Letters* **58,** 51–66.

Metcalf, R. V., Smith, E. I., Walker, J. D., Reed, R. C. & Gonzales, D. A., 1995. Isotopic disequilibrium among commingled hybrid magmas: evidence for a two-stage magma mixing–commingling process in the Mt. Perkins Pluton, Arizona. *Journal of Geology* **103,** 509–527.

Moecher, D. P., Essene, E. J. & Anovitz, L. M., 1988. Calculation and application of clinopyroxene–garnet–plagioclase–quartz geobarometers. *Contributions to Mineralogy and Petrology* **100,** 92–106.

Montel, J.-M., Didier, J. & Pichavant, M., 1991. Origin of surmicaceous enclaves in intrusive granites. In: Didier, J. & Barbarin, B. (eds) *Enclaves and Granite Petrology.* Amsterdam: Elsevier, pp. 509–528.

Moreno-Ventas, I., Rogers, G. & Castro, A., 1995. The role of hybridization in the genesis of Hercynian granitoids in the Gredos Massif, Spain: inferences from Sr–Nd isotopes. *Contributions to Mineralogy and Petrology* **120,** 137–149.

Munksgaard, N. C., 1988. Source of the Cooma granodiorite, New South Wales—a possible role of fluid–rock interactions. *Australian Journal of Earth Sciences* **35,** 363–377.

Newton, R. C. & Haselton, H. T., 1981. Thermodynamics of the garnet–plagioclase–Al_2SiO_5–quartz geobarometer. In: Newton, R. C., Navrotsky, A., Wood, B. J. (eds) *Thermodynamics of Minerals and Melts.* Springer: New York, pp. 131–147.

Nicholls, I. A., 1974. A direct fusion method of preparing silicate rock glasses for energy-dispersive electron microprobe analysis. *Chemical Geology* **14,** 151–157.

Perkins, D. & Chipera, S. J., 1985. Garnet–orthopyroxene–plagioclase–quartz barometry: refinement and application to the English River Subprovince and the Minnesota River Valley. *Contributions to Mineralogy and Petrology* **89,** 69–80.

Phillips, G. N., Wall, V. J. & Clemens, J. D., 1981. Petrology of the Strathbogie batholith: a cordierite-bearing granite. *Canadian Mineralogist* **19,** 47–64.

Pichavant, M., Hammouda, T. & Scaillet, B., 1996. Control of redox state and Sr isotopic compositions of granitic magmas: a critical evaluation of the role of source rocks. *Transactions of the Royal Society of Edinburgh* **87,** 321–329.

Pin, C., Binon, M., Belin, J. M., Barbarin, B. & Clemens, J. D., 1990. Origin of microgranular enclaves in granitoids: equivocal Sr–Nd evidence from Hercynian rocks in the Massif Central (France). *Journal of Geophysical Research* **95,** 17821–17828.

Pitcher, W. S., 1991. Synplutonic dikes and mafic enclaves. In: Didier, J. & Barbarin, B. (eds) *Enclaves and Granite Petrology.* Amsterdam: Elsevier, pp. 383–391.

Poli, G. E. & Tommasini, S., 1991. Model for the origin and significance of microgranular enclaves in calk-alkaline granitoids. *Journal of Petrology* **32,** 657–666.

Poli, G., Tommasini, S. & Halliday, A. N., 1996. Trace element and isotopic exchange during acid–basic magma interaction processes. *Transactions of the Royal Society of Edinburgh* **87,** 225–232.

Powell, C. McA., 1984. Ordovician–Early Carboniferous. In: Veevers, J. J. (ed.) *Phanerozoic Earth History of Australia.* Oxford: Oxford University Press, pp. 290–340.

Powell, R. & Holland, T. J. B., 1987. An internally consistent thermodynamic dataset with uncertainties and correlations: 3. Applications to geobarometry, worked examples and a computer program. *Journal of Metamorphic Geology* **6,** 173–204.

Price, R. C., 1983. Geochemistry of a peraluminous granitoid suite from NE Victoria, SE Australia. *Geochimica et Cosmochimica Acta* **47,** 31–42.

Reid, J. B., Jr & Hamilton, A. M., 1987. Origin of Sierra Nevadan granite: evidence from small scale composite dikes. *Contributions to Mineralogy and Petrology* **96,** 441–454.

Richards, J. R. & Singleton, O. P., 1981. Palaeozoic Victoria, Australia: igneous rocks, ages and their interpretation. *Journal of the Geological Society of Australia* **28,** 395–421.

Ringwood, A. E., 1955.The geology of the Deddick–Wulgulmerang area, East Gippsland. *Proceedings of the Royal Society of Victoria* **34,** 238–246.

Roddick, J. C. & Compston, W., 1977. Strontium isotopic equilibration: a solution to a paradox. *Earth and Planetary Science Letters* **60,** 293–304.

Rossiter, A. G., 1994. The substrate of the Lachlan Fold Belt as inferred from granite compositions. *12th Australian Geological Convention, Perth, GSA Abstracts No. 37.* Perth: University of Western Australia, p. 383.

Salje, E. & Wernecke, C., 1982. The phase equilibrium between sillimanite and andalusite as determined from lattice vibrations. *Contributions to Mineralogy and Petrology* **79,** 56–76.

Sawyer, E. W., 1996. Melt segregation and magma flow in migmatites: implications for the generation of granite magmas. *Transactions of the Royal Society of Edinburgh* **87,** 85–94.

Sen, S. K. & Bhattacharya, A., 1984. An orthopyroxene–garnet thermometer and its application to the Madras charnockites. *Contributions to Mineralogy and Petrology* **88,** 64–71.

Spear, F. S., 1993. *Metamorphic Phase Equilibria and Pressure–Temperature–Time Paths.* Washington, DC: Mineralogical Society of America, 799 pp.

Steele, D. A., Price, R. C., Fleming, P. D. & Gray, C. M., 1991. The origin of Cooma Supersuite granites: source protoliths and early magmatic processes. *2nd Hutton Symposium, Canberra, Abstracts.* Canberra: Bureau of Mineral Resources, p. 100.

Tatsumi, Y. & Ishizaka, K., 1982. Origin of high-magnesian andesites in the Setouchi volcanic belt, SW Japan, 1: Petrographic and chemical characteristics. *Earth and Planetary Science Letters* **60,** 293–304.

Taylor, R. S. & McLennan, S. M., 1985. *The Continental Crust: its Composition and Evolution.* Oxford: Blackwell Scientific Publications.

Tsuchiyama, A., 1985. Dissolution kinetics of plagioclase in the melt of the system diopside–albite–anorthite, and origin of dusty plagioclase in andesites. *Contributions to Mineralogy and Petrology* **89,** 1–16.

Vernon, R. H., 1983. Restite, xenoliths and microgranular enclaves in granites. *Journal of Proceedings of the Royal Society of New South Wales* **116,** 77–103.

Vernon, R. H., 1984. Microgranular enclaves in granites—globules of hybrid magma quenched in a plutonic environment. *Nature* **309,** 438–439.

Vernon, R. H., 1990. Crystallization and hybridism in microgranular enclave magmas: microstructural evidence. *Journal of Geophysical Research* **95,** 17849–17859.

Wall, V. J., Clemens, J. D. & Clarke, D. B., 1987. Models for granitoid evolution and source compositions. *Journal of Geology* **95,** 731–748.

White, A. J. R. & Chappell, B. W., 1983. Granitoid types and their distribution in the Lachlan Fold Belt, SE Australia. *Geological Society of America Memoir* **159,** 21–34.

White, A. J. R. & Chappell, B. W., 1988. Petrology of igneous rocks. In: Douglas, J. G. & Ferguson, J. A. (eds) *Geology of Victoria.* Melbourne: Geological Society of Australia, Victorian Division, pp. 427–439.

White, A. J. R., Chappell, B. W. & Wyborn, D., 1991. Enclaves of S-type granites in the Lachlan Fold Belt, southeastern Australia. In: Didier, J. & Barbarin, B. (eds) *Enclaves and Granite Petrology*. Amsterdam: Elsevier, pp. 493–507.

Williams, I. S., 1992. Some observations on the use of U–Pb zircon geochronology in the study of granitic rocks. *Transactions of the Royal Society of Edinburgh, Earth Sciences* **83,** 447–458.

Williams, I. S., Compston, W. & Chappell, B. W., 1983. Zircon and monazite U–Pb systems and the histories of I-type magmas, Berridale Batholith, Australia. *Journal of Petrology* **24,** 76–97.

Wyborn, L. A. I. & Chappell, B. W., 1983. Chemistry of the Ordovician and Silurian greywackes of the Snowy Mountains, SE Australia: an example of chemical evolution of sediments with time. *Chemical Geology* **39,** 81–92.

Wyborn, D., Chappell, B. W. & Johnston, R. M., 1981. Three S-type volcanic suites from the Lachlan Fold Belt, SE Australia. *Journal of Geophysical Research* **86,** 10335–10348.

Wyborn, D., White, A. J. R. & Chappell, B. W., 1991. Enclaves in the S-type Cowra Granodiorite. *Excursion Guide. 2nd Hutton Symposium on Granites, Canberra.* Canberra: Bureau of Mineral Resources.